GAS CLEANING STUDIES OF U. S. BUREAU OF MINES INCINERATORS

Stack Effluent Tests on BOMAEC-30 and BOMAEC-100 Incinerators

Richard Dennis, Charles E. Billings, William R. Samples and Leslie Silverman

Air Cleaning Laboratory
School of Public Health
Harvard University
Boston, Massachusetts

SUMMARY

Representative stack samples were collected during seven incineration tests on the BOMAEC-30 incinerator and five tests on the BOMAEC-100 unit. Sawdust burnings were made in both incinerators to (1) compare their performance and (2) to evaluate the effect of design changes in the BOMAEC-30 unit. Office waste ranging in moisture content from 10 to 50 percent was burned in the incinerators to study combustion efficiency. Both units produced similar effluents when burning like charges and indicated the desirability of further improvements in combustion before design of final air cleaning systems. On a basis of sawdust tests the BOMAEC-100 incinerator yielded better overall combustion efficiency. Although the BOMAEC-30 appeared to do a better job in burning waste, the comparison is clouded by unavoidable differences in charge composition.

INTRODUCTION

At the request of the Division of Engineering, Atomic Energy Commission (Dr. Joseph A. Lieberman) arrangements were made to have the Harvard University Air Cleaning Laboratory conduct stack sampling and gas cleaner evaluation tests on two special incinerators developed by the Combustion Research Section, U. S. Bureau of Mines, Pittsburgh, Pa., the BOMAEC-30 unit, designed for the disposal of radioactive waste materials from hospitals and research laboratories and the BOMAEC-100 unit for similar disposal of somewhat larger volumes.

Stack sampling was conducted at the Bureau of Mines Combustion Research Laboratory, Pittsburgh, Pa., from November 29 through December 3, 1954 and June 8 through June 14, 1955 by staff members of the Harvard University Air Cleaning Laboratory. Incinerator operation and apparatus for supplying a continuous record of the combustion process was supervised by Mr. Cecil H. Schwartz of the Combustion Research Section.

The objectives of the first test program (1954) were (1) to establish air cleaning requirements for the BOMAEC-30 incinerator through the determination of concentration, size, and approximate composition of the incinerator effluent and (2) to evaluate the over-all performance of the originalair cleaning system consisting of a centrifugal section followed by glass filter bags.

Five sawdust incineration tests were made in which the quantity of charge, burning time, over-fire air flow rate and incineration temperature were essentially constant.

Analyses of combustion and sampling data for the BOMAEC-30 unit as first tested indicated a sooty effluent during the first fifteen to twenty minutes of the combustion cycle which caused rapid plugging

of glass filter bags. Condensation of volatile organic materials in the stack gas after passing through the glass bags produced tar droplets which could not have been filtered economically by an AEC absolute-type filter. Pressure loss through the glass bags increased rapidly during the first stages of combustion but remained constant during the last 20 to 30 minutes of operation, indicating that the organic constituents were the primary cause of bag plugging (Figure 1). The deposition of tars in the Ross tubular heat exchanger (which reduced cooling capacity) in conjunction with a fairly high pressure loss suggested that a simple spray tower might be substituted as a more effective means of precooling the stack gas.

As a result of these tests arrangements were made to increase the depth of the combustion chamber and adjust the air supply through changes in either slot width or air volume. The above modifications were based upon the following data: (a) the length to diameter ratio of the BOMAEC-30 combustion chamber was smaller and the Reynold's number through the air entry slots lower than those considered optimum in earlier studies on a smaller pilot plant incinerator (1).

The Air Cleaning Laboratory supplied a pneumatic spray nozzle which was installed in a spray cooling tower (in place of the present tubular heat exchanger). It was also agreed that typical waste charges should be prepared for the BOMAEC-30 unit in addition to sawdust charges so that a more realistic picture of field performance could be drawn.

The objectives of the second test series were (1) to determine whether any improvement in combustion would be realized through design changes in the BOMAEC-30 incinerator, (2) to determine

performance of the BOMAEC-30 unit in burning both rubbish and sawdust charges and (3) to determine the combustion characteristics with sawdust and rubbish and the composition and concentration of effluent gas from the BOMAEC-100 incinerator.

This report includes the results of seven combustion tests (five sawdust and two office waste charges) upon the BOMAEC-30 incinerator and five tests (three sawdust and two office waste charges) upon the BOMAEC-100 unit.

BOMAEC-30 INCINERATOR

A. Description

Figure 2 shows the original form of the BOMAEC-30 incineration and air cleaning equipment. Major design changes, based upon results of previous stack sampling, included an eighteen inch extension of the combustion chamber and a reduction in the width of the air entry slots from $\frac{1}{4}$ to 3/16 inches. No change was made in the position of the air preheat jacket, as shown in Figure 3, so that the preheating zone remained as in the original design. Minor changes in the location of the metering system for supply air have not been shown since they had no bearing upon incinerator performance.

A vertical 4 ft. by 6 in. diameter steel pipe with a pneumatic spray nozzle (Figure 3), directed concurrently, was substituted for the Ross heat exchanger employed in the original gas cooling system. Gas sampling points in the incinerator stack and at the spray tower exit were the same as in previous tests. Oxygen and carbon dioxide concentrations were measured upstream of the water spray system. Gas temperatures were measured in the same locations as in previous tests or as noted in Figure 3.

B. Physical Condition

Prior to testing, the incinerator outlet pipe was blown out to remove a small deposit of ash. No condensate or significant amount of ash or tarry residue appeared in the spray tower drain line. Substitution of the spray tower for the tubular heat exchanger permitted greater air flows than the original system. Glass bags were employed in most tests. Although bag pressure loss increased during each test to maximum values of approximately 9 inches of water, it was possible to maintain desired air flow rates throughout all tests.

STACK SAMPLING EQUIPMENT AND PROCEDURE

A. Stainless Steel Probes and Glass Filters

Particulate samples from the incinerator and spray tower outlet pipes were collected on 1½ inch diameter glass filter circles* supported in a stainless steel filter holder (constructed by machining flat, recessed surfaces on a standard 1" stainless steel union). A ½" diameter, 16" long, straight, steel probe was attached to the filter holder (Figure 4) and inserted in the incinerator outlet duct (Figure 3) so that the tip of the probe faced the gas stream. A similar holder and probe (9" long) was inserted in the tee fitting downstream of the spray tower (Figure 3). The gaseous effluent from the upstream filter holder was drawn through a 4', water cooled, condenser prior to passing through the flowmeter and sampling pump. Cooling was required to protect rubber fittings from high gas temperatures (1100 to 1500°F). Sampling rates were adjusted so that the entry velocities were nearly isokinetic by applying standard temperature and pressure corrections to the flowmeter calibrations. However, rapid filter plugging during some tests and uncontrollable variations in incinerator air flow caused some deviation from isokinetic sampling velocity.

B. Bacharach Stain Tests

Concurrent stain tests were made by the Bureau Combustion Research Laboratory on the incinerator stack gas with a Bacharach smoke indicator. Density of the smoke stains (which are on record at the Combustion Research Laboratory) showed excellent agreement with the appearance of samples collected upon the all-glass filters. No attempt was made during the current test series to sample the glass bag effluent. Bag pressure loss measurements and metering of total air flow were conducted as reported previously.

* Type 1106 B Glass Paper, Mine Safety Appliances Co., Pittsburgh, Pa.

SAMPLING AND TEST RESULTS - BOMAEC-30 INCINERATOR

A. Sawdust Charge

Eight combustion tests on the BOMAEC-30 incinerator (PH-7 through PH-14) were conducted as in the previous survey. Coarse sawdust was dumped into the combustion chamber, levelled by hand, and ignited with a kerosene soaked rag. Typical results (representing tests PH-7 to PH-11) for the combustion of 25 pound sawdust charges at rated air flow (approximately 60 cfm) are shown graphically in Figure 5. Although sawdust charges were smaller than those used in earlier tests (33 pounds) these data indicate that no important changes in effluent concentrations (0.1 to 0.5 gr./cu.ft. STP) or incineration temperatures (1400° - 1500°F) were produced by structural changes in the incinerator, i.e. lengthened combustion chamber and reduced air slot width.

Incinerator stack temperatures rose to slightly higher levels (1300° - 1500°F) due to increased air flow (approximately 10 percent more than in December tests) and a slight reduction in organic components was noted in the stack gas effluent during the first 10 minutes of operation. However, the change in combustible concentrations became insignificant when the periods of organic-free effluent were compared on a basis of total burning time. It should be noted that gas samples collected downstream of the spray cooling system (which showed a higher organic loading) furnished a more accurate picture of effluent composition since condensed tars, some of which passed through sampling filters in the volatile phase at high temperatures, were removed from the cooled gas.

An attempt to improve combustion efficiency through increased air flow, approximately 75 cfm, proved unsuccessful as shown by the

increased organic content of the ash (60 percent). This substantiated the results of past tests by the Combustion Research Laboratory where Bacharach smoke stains had been used to evaluate combustion efficiency. Stack temperature rose to a higher level (1700°F) and the total combustion period was reduced to 25 minutes. Increased combustible loadings were attributed to shortened particulate retention time and changed air flow distribution within the incinerator.

B. Waste Charge

Tests PH-12 and PH-13 represent the combustion of 60 pound charges of office waste consisting of miscellaneous paper, cardboard, and lunch refuse. Estimated moisture contents in tests PH-12 and PH-13 were 10 to 15 percent and 50 percent, respectively, on a dry basis. Combustion of the drier charge (10 to 15 percent moisture) followed the general temperature pattern of the sawdust charges although the average effluent loadings were higher (0.6 gr./cu.ft.) and contained much less combustible material (3 percent). The reduction of distillable combustibles in the charge (primarily cellulose and mineral fillers) accounted for the improved state of the stack effluent. Maximum bag pressure loss during this test was 8.6 inches as compared to 9.5 inches of water for sawdust runs.

A similar waste charge containing 50 percent moisture (Figure 6) showed unsatisfactory performance in that (1) ignition difficulties were experienced and (2) incineration temperatures did not climb to a high enough level to completely burn the entrained combustible materials. Average effluent loadings showed approximately 60 percent combustibles. Bag pressure loss, however, did not exceed the average value of 9.4 inches of water noted for sawdust. At the completion of this test some 16 pounds of ash and unburned charge remained in the incinerator.

BAG PRESSURE LOSS

Pressure loss through the glass bags reached fairly high values during each combustion test (9.5 inches of water). However, pressure loss reduced to approximately 1.8 inches of water at 60 cfm following bag shaking (25 raps) and did not appear to build up to higher base levels during successive tests. The glass bags were removed from the BOMAEC-30 unit at the end of the tests and shaken into a barrel to examine the deposited material. Nearly two pounds of fine ash were dislodged from the bags which indicated that the mechanical shaking mechanism may not be as effective as it should be. The surface of the bags did not show the heavy soot stain observed in previous tests.

SPRAY NOZZLE PERFORMANCE

The pneumatic atomizing nozzle* located in the cooling tower had sufficient capacity at maximum rated flow (9.7 gal./hr.) to reduce stack temperatures from 1400°F to 200°F when air flow rates did not exceed 55 to 65 cfm. However, maximum water rates were not employed in most tests since cooling to 400°F was considered adequate by Mr. Schwartz. It was noted that cooling capacity was exceeded only during test PH-14 when a high air flow rate was used (approximately 80 cfm) which elevated stack temperatures to 1700°F.

* Spraying Systems Company, Bellwood, Illinois
Nozzle 22B - Water pressure 10-60 psi; Air pressure 10-70 psi.

BOMAEC-100 INCINERATOR

A. Description

A schematic drawing of the BOMAEC-100 incinerator (Figure 7) shows the location of the stack sampling probe, the sampling points for the oxygen and carbon dioxide recorders and Bacharach smoke indicator, and the location of the thermocouples.

Supply air for these tests was delivered under positive pressure by a turbo-compressor and entered the combustion chamber through six tangential inlets. Hot gases were exhausted through the incinerator stack at the top of the unit. Although the effluent would, in practice, pass through filtration equipment, the hot gases were vented to an open hood since the primary purpose of the current tests was to evaluate stack gas particulate composition and concentration.

B. Physical Condition

Before any tests were conducted on this unit it was determined that no ash deposits existed in the combustion chamber and stack. According to Mr. Schwartz, incineration and recording apparatus were functioning properly and duplicated operating conditions of previous tests.

C. Stack Sampling Equipment and Procedure

Only incinerator stack samples were collected during tests on the BOMAEC-100 unit. Sampling apparatus was identical with that used in testing the BOMAEC-30 except for a 90° bend in the sampling probe which allowed it to face into the hot gas stream. Again, simultaneous stain tests were run by the Combustion Research Laboratory with a Bacharach smoke indicator. The incinerator air flow for these tests was metered cold at the compressor inlet. Since the flow meter and the compressor handled standard air, delivered volume was nearly constant during each test.

SAMPLING AND TEST RESULTS - BOMAEC-100 INCINERATOR

A. Sawdust Charge

Five combustion tests were conducted on the BOMAEC-100 incinerator (PH-15 through PH-19). The incinerator was charged by placing 20 separate, five pound cardboard containers of sawdust in the combustion chamber. The charge was then ignited by an auxiliary gas burner. Tests PH-15 and PH-18 were conducted at an air flow of 155 cfm (700 pounds per hour) and PH-16 at 193 cfm (870 pounds per hour). The inlet air was not preheated as in the BOMAEC-30 incinerator and the slight temperature rise was due to the heat of compression. The indicated burning period was decreased from approximately 80 minutes (test PH-18) to 60 minutes (test PH-16) by the increase in air flow. Incinerator stack temperatures rose to slightly over 1300°F in the low air flow tests and to 1500°F in the high air flow test. Oxygen concentrations in the stack gas fell to very low values, less than 0.5 percent, for the low air flow tests and to 0.5 percent for the high air flow tests. Conversely, the carbon dioxide curves showed maximum concentrations of about 18 percent for corresponding times. During the runs it was noted that sparks were emitted from the stack when total dust loadings were at maximum levels.

Stack loadings for these tests as obtained from the samples collected on all-glass filter circles are reported graphically along with the other operating data. Figure 8 (test PH-18) shows that for an air flow of 155 cfm the total dust loadings varied from 0.20 to 0.52 gr./cu.ft. while the combustible loadings varied from 0.0 to 0.20 gr./cu.ft. By increasing the air flow to 193 cfm the total dust concentrations ranged from 0.18 to 1.7 gr./cu.ft. while the combustible loadings varied from 0.0 to 0.45 gr./cu.ft. The high loading values

for the high air flow rate occurred at the end of the test after the oxygen concentration had returned to 21 percent; this may have been due to the entrainment of a large amount of partially burned material after the actual combustion had ceased.

It appeared that increased air flow did not improve combustion since total combustible effluent was increased. This confirms the results of similar tests on the BOMAEC-30 incinerator.

B. Waste Charge

Test PH-19 (Figure 9) represents the combustion of 112 pounds of office waste (20 percent moisture) at an air flow of 155 cfm (700 pounds per hour) and test PH-17 represents 101 pounds of office waste (10-15 percent moisture) at an air flow of 193 cfm (870 pounds per hour) in the BOMAEC-100 incinerator. The loose waste charge was dumped into the incinerator and ignited as before with an auxiliary gas burner. The estimated burning period was shortened by about 15 minutes with increased air flow. However, minimum oxygen concentrations were 2.5 percent at the low flow rate (155 cfm) in contrast to 0.4 percent at the high flow rate (193 cfm). Stack temperatures were consistent with reported oxygen concentrations in tests PH-19 and PH-17, i.e., the greater the temperature the lower the oxygen concentration. However, temperatures dropped below 1200°F for the last two-thirds of the runs. Reduced burning rate and greater excess oxygen in test PH-19 was attributed to possible differences in charge composition and bulk density. A series of violent smoke puffs were expelled from the incinerator stack for the first 5 minutes of both tests. Mr. Schwartz attributed this to rapid combustion of printers cleaning rags, film, or other highly volatile materials in the charge. The dust loadings, based upon stack samples, showed a great dependence on air flow. Test PH-19 (air flow 155 cfm) showed dust

loadings ranging from 0.5 to 1.2 gr./cu.ft. with an average value of approximately 0.9 gr./cu.ft. When the flow rate was increased to 193 cfm (test PH-17) the total loading rose to 5.9 gr./cu.ft. at one point and averaged approximately 2.0 gr./cu.ft. for the entire run. The average combustible loading was nearly three times greater when air flow rate was increased to 193 cfm from 155 cfm (0.27 to 0.78 gr./cu.ft.). These data conform to the performance of the BOMAEC-30 incinerator when recommended air flows were exceeded.

PERFORMANCE COMPARISON
BOMAEC-30 AND BOMAEC-100 INCINERATORS

Table I summarizes the comparative performance of the BOMAEC-30 and BOMAEC-100 incinerators for sawdust and waste burning. Columns 1, 2 and 3 indicate total weight of charge, air flow rate and ratio of air flow to charge, respectively; column 4, the burning rate in lbs./hr; columns 5 and 6, the stack emission in terms of total and combustible materials emitted in lbs./hr./lb. of charge; and column 7, the percent combustibles in the stack effluent.

Air flow rates in excess of those recommended by the Combustion Research Laboratory resulted in increased stack emission of both mineral and combustible materials although burning rates were increased by about 20 percent.

Over-all combustion efficiency of the BOMAEC-100 unit appeared better than that of the BOMAEC-30 unit with sawdust. Combustible loadings were equal to or less than those of the BOMAEC-30 unit, the air to charge ratio lower and the burning rate approximately 65 percent greater. However, waste combustion tests indicated a lower stack emission with the BOMAEC-30 unit at the expense of a lower burning rate and greater air to charge ratio.

A higher moisture content and possible variation in composition in the waste may have accounted for the increased stack emission in the case of rubbish charges in the BOMAEC-100 unit.

Based solely upon sawdust tests it appeared that the arrangement of air jets within the BOMAEC-100 unit may have been responsible for its improved combustion. It should be noted, however, that since no preheating of inlet air took place in the BOMAEC-100 incinerator, the combustion conditions should have been less favorable than in the BOMAEC-30 unit.

TABLE I

Comparative Performance of BOMAEC-30 and BOMAEC-100 Incinerators

Total Charge lbs.	Air Flow Rate cfm	Air to Charge Ratio cfm/lb.	Burning Rate lbs./hr.	Stack Emission Rate		Percent Combustibles in Stack Effluent
				Total lbs./hr./lb. of charge	Combustible lbs./hr./lb. of charge	
A. BOMAEC-30; SAWDUST CHARGE						
25	60	2.4	45	0.0033	0.0011	33.3
25	79	3.2	65	0.012	0.0075	62.3
B. BOMAEC-30; WASTE CHARGE (10-15% MOISTURE)						
60	63	1.05	33*	0.0043	0.00016	3.8
C. BOMAEC-30; WASTE CHARGE (50% MOISTURE)						
69	63	0.91	22*	0.0071	0.0047	66.2
D. BOMAEC-100; SAWDUST CHARGE						
100	155	1.55	75	0.0043	0.0011	25.2
100	193	1.93	100	0.012	0.0023	18.8
E. BOMAEC-100; WASTE CHARGE (10-20% MOISTURE)						
100	155	1.55	75	0.012	0.0035	29.4
112	193	1.72	124	0.030	0.011	37.4

* Burning rate based upon weight of dry charge completely burned.

CONCLUSIONS

A. BOMAEC-30 Incinerator

1. The substitution of a high pressure water spray* for the Ross heat exchanger provides better control of gas cooling and reduces the over-all pressure loss in the gas cleaning system.

2. Glass bags still do not constitute an effective gas pre-cleaner for AEC type absolute filters due to the presence of tar droplets and water vapor in the gas stream. Resistancewise, glass bags may be serviceable provided that sufficient fan capacity is available.

3. Increasing the height of the burning chamber and reducing the width of the air inlet slots makes no significant change in the concentration and physical nature of the stack effluent for sawdust combustion tests. Temperatures, oxygen concentrations and burning rates were essentially the same as in previous tests.

4. Increasing air flow rate shortens the overall burning time but produces higher stack loadings containing a greater percentage of combustibles. These data agree with past smoke stain tests of the Combustion Research Laboratory.

5. Burning of comparatively dry materials (10-15 percent moisture) or other cellulose type wastes results in a substantially lower emission of combustible materials than found for sawdust. However, the burning rate and uniformity of combustion is largely dependent upon the bulk density of the charge.

6. Burning of wet waste (50 percent moisture on a dry basis) which simulates the water content of some biological wastes, is unsatisfactory. The burning rate was low, stack temperatures were

* Spraying Systems Company, Bellwood, Illinois
Nozzle 22B; Water pressure, 10-60 psi; Air pressure, 10-70 psi.

below 1000°F for most of the test and the quantity of combustible material leaving the stack was about thirty times greater than that from low moisture content waste.

B. BOMAEC-100 Incinerator

1. Incomplete combustion of sawdust occurs during the first 10 to 20 minutes of tests conducted at rated air flow (155 cfm) due to oxygen deficiency and rapid distillation of volatiles. During the last half of each test, stack temperatures dropped to less than 1200°F, below which level combustion is not considered optimum.

2. The concentrations of combustible materials in the stack effluent present the same gas cleaning problems posed by the BOMAEC-30 incinerator.

3. Sawdust combustion in the BOMAEC-100 incinerator appears more efficient than in the BOMAEC-30 unit based upon (1) equal or slightly lower stack emissions, (2) lower air to charge ratio, and (3) increased burning rate. Better performance may have been due to differences in method of air introduction and in air flow pattern within the incinerator.

4. Combustion of office waste (16 - 20 percent moisture) is less efficient than that of sawdust. Combustible effluent loadings were about three times higher than those of sawdust and stack temperatures dropped below 1200° for the last two-thirds of each test.

5. Combustion of both sawdust and waste is not improved by increasing air flow, i.e. 193 cfm vs. 155 cfm (the recommended flow rate). Although burning rate was increased in both cases by about 30 percent, the total weight of combustible effluent was increased about five times for the same quantity of charge.

RECOMMENDATIONS

A. BOMAEC-30 Incinerator

1. Operational and constructional changes in the BOMAEC-30 incinerator merit further consideration since tests with wet rubbish (50 percent moisture content) indicate unsatisfactory combustion. Since increased air flow did not improve combustion it is suggested that a change in the number and arrangement of air inlets be considered.

2. Preliminary drying of wet charges should be investigated if no auxiliary burners are to be employed. Combustion temperatures with wet waste were far below the level required for complete burning of airborne particulates.

3. If no further mechanical improvements can be made, the intermittent use of an after-burner to maintain a 1200°-1400°F stack temperature still appears as a practical way to reduce combustible loadings.

4. Recommendations for a final gas cleaning system, assuming that present combustion conditions are optimum, remain as reported previously. Following passage through a spray cooler and reheating (to prevent further condensation of water) cooled gases can be filtered through a mineral wool roughing filter to remove a large percentage of the organic materials. Final gas cleaning units would again consist of glass bags followed by absolute filters.

B. BOMAEC-100 Incinerator

1. Recommendations to improve combustion in the BOMAEC-100 incinerator follow the same pattern as for the BOMAEC-30 unit. Since limited test data for both sawdust and waste combustion show reduced emission of combustibles at lower air flow rates, it seems reasonable to consider a further reduction in total air flow.

2. Gas cleaning equipment for the BOMAEC-100 incinerator must necessarily be comparable to that of the BOMAEC-30 unit.

LITERATURE CITED

(1) R. C. Corey, L. A. Spano, C. H. Schwartz, and Harry Perry. "Experimental Study of Effects of Tangential Overfire Air on the Incineration of Combustible Wastes", Air Repair, vol. 3, no. 2, November, 1953.

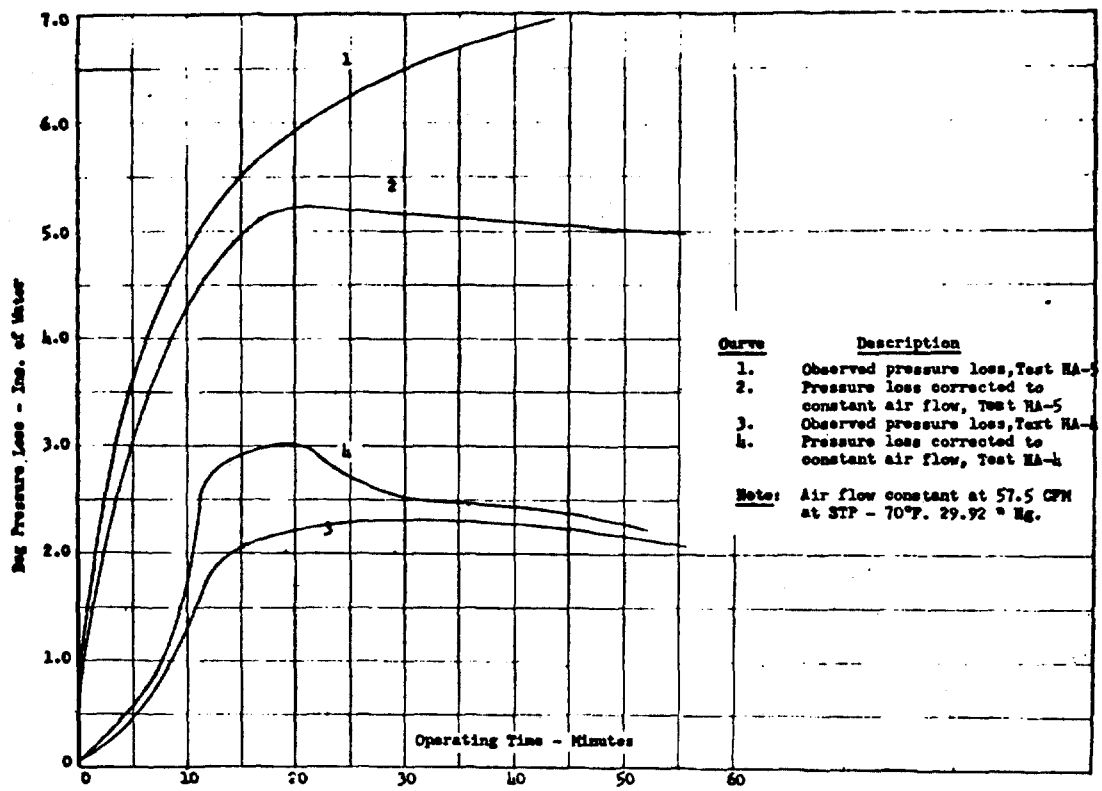

Fig. 1--Pressure Loss Increase Through Glass Bags During Incineration Tests.

FIGURE 2 - LEGEND

1. Incinerator (29" Inside Diameter, 29 1/2" High)
2. Air Inlet, Metered by 2" Orifice in 4" Pipe
3. Incinerator Inlet Static Pressure Tap
4. Sight Glass for Observing Combustion
5. Pre-Heat Air (Jacket) Temperature, Thermocouple Nos. 1 and 4
6. Incinerator Outlet Gas Temperature, Thermocouple No. 3
7. Incinerator Outlet Static Pressure Taps
8. Incinerator Outlet Sampling Probe
9. Gas Temperature Entering Heat Exchanger, Thermocouple No. 6
10. Inlet to Heat Exchanger Static Pressure Tap
11. Ross Heat Exchanger
12. Cooling Water Inlet and Outlet
13. Heat Exchanger Outlet Static Pressure Taps
14. Gas Sampling Tube to Oxygen Recorder
15. Gas Sampling Tube to Carbon Dioxide Recorder
16. Drain Plug, Condensate from Stack Gas
17. Heat Exchanger Sampling Probe
18. Bag House (Seven Glass Cloth Bags)
19. Final CC-6 Filter Housing (No Filters Used)
20. Buffalo Fan
21. Ash Drums (35 Gallon Size)
22. Sampling Probe to High Volume Sampler
23. Temperature After Fan, Thermocouple Nos. 2 and 5
24. Bag Pressure Loss Taps
25. Fan Static Pressure Tap

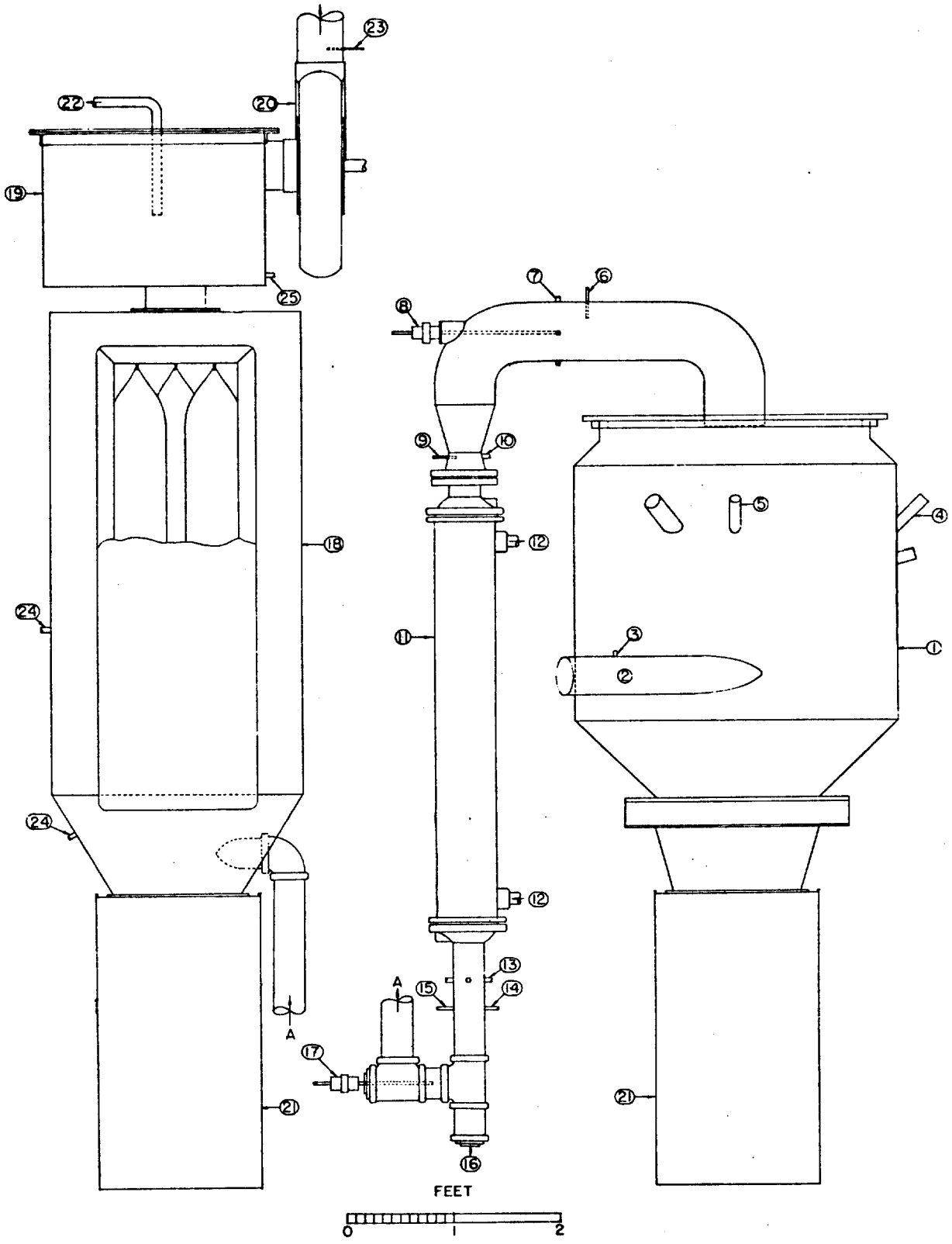

Fig. 2--Schematic Drawing of Institutional Incinerator (BOMAEC-30) Showing Sampling Points.

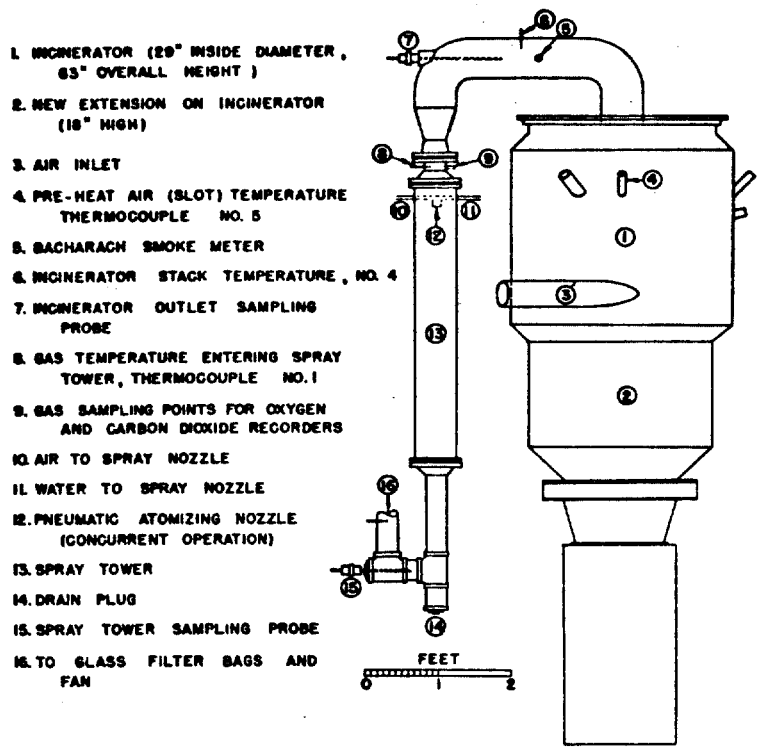

Fig. 3--Schematic Drawing of Revised Institutional Incinerator (BOMAEC-30) Showing Sampling Points.

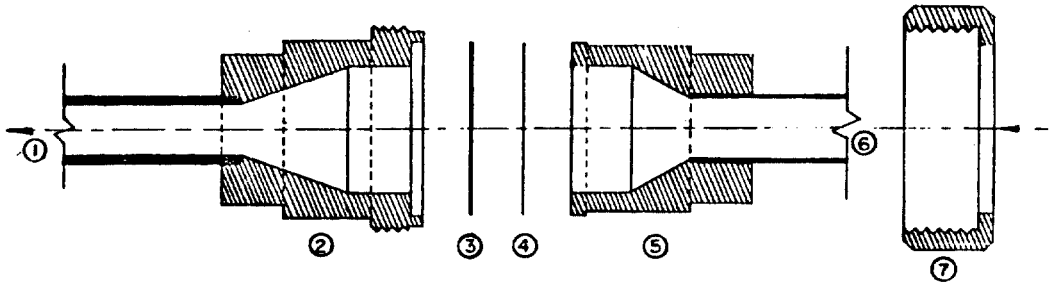

1 TO FLOW METER AND PUMP
2 1" STD. STAINLESS STEEL UNION - REAR HALF
3 BACKER SCREEN
4 ALL GLASS FILTER CIRCLE
5 1" STD. STAINLESS STEEL UNION - FRONT HALF
6 SAMPLING PROBE EXTENSION
7 UNION NUT

INCHES
0 1 2 3 4

Fig. 4--Stainless Steel Sampling Probe and Holder for All Glass Filter Circles.

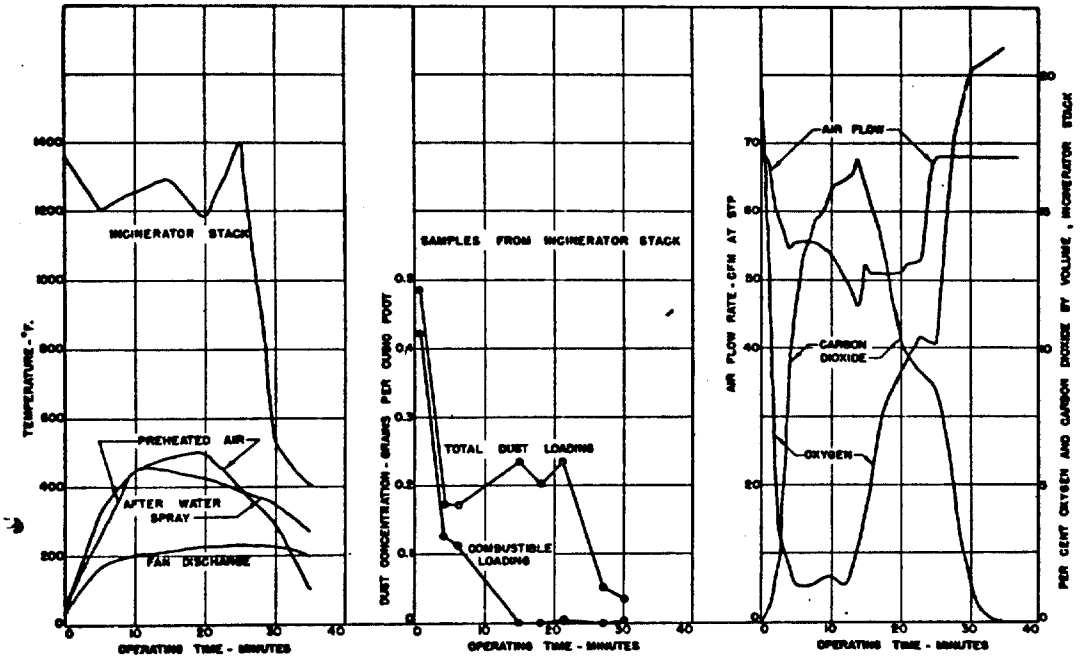

Fig. 5--Test Data, Test PH-8, 25 Lbs. Sawdust in BOMAEC-30.

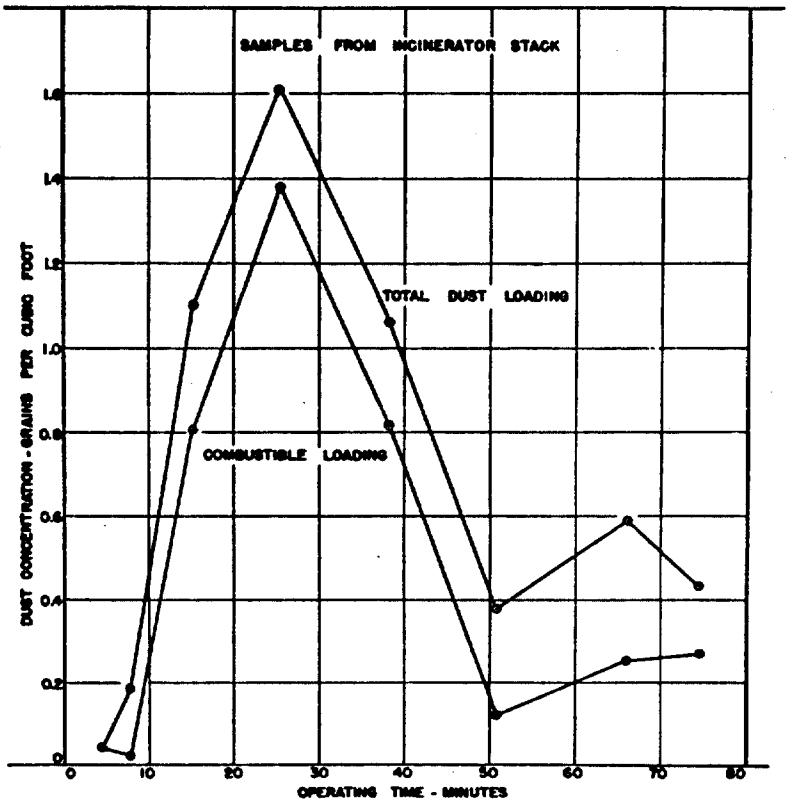

Fig. 6--Test Data, Test PH-13, 69 Lbs. Office Waste with 50% Moisture in BOMAEC-30.

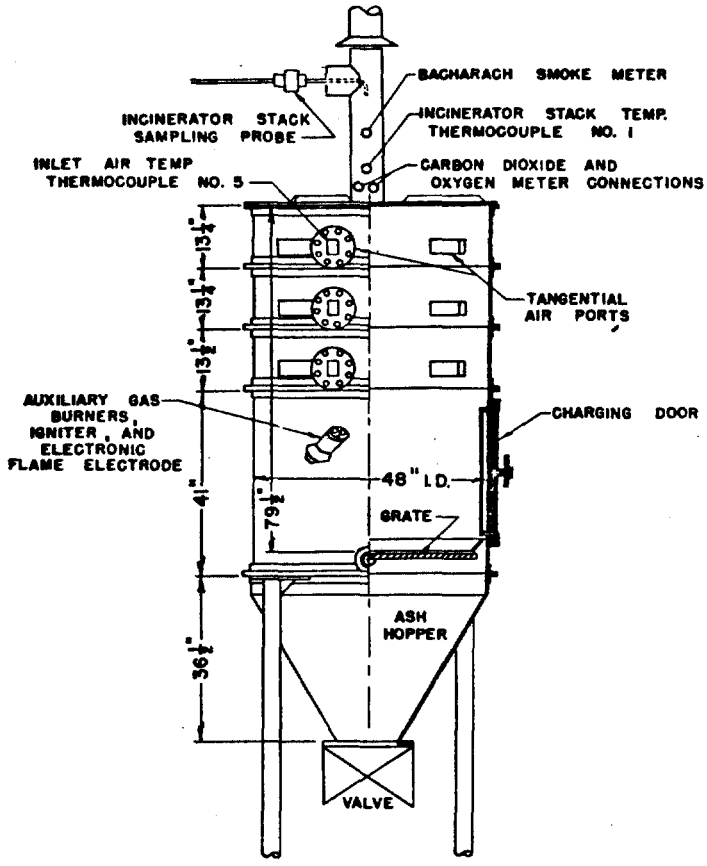

Fig. 7--Schematic Drawing of BOMAEC-100 Incinerator Showing Sampling Point.

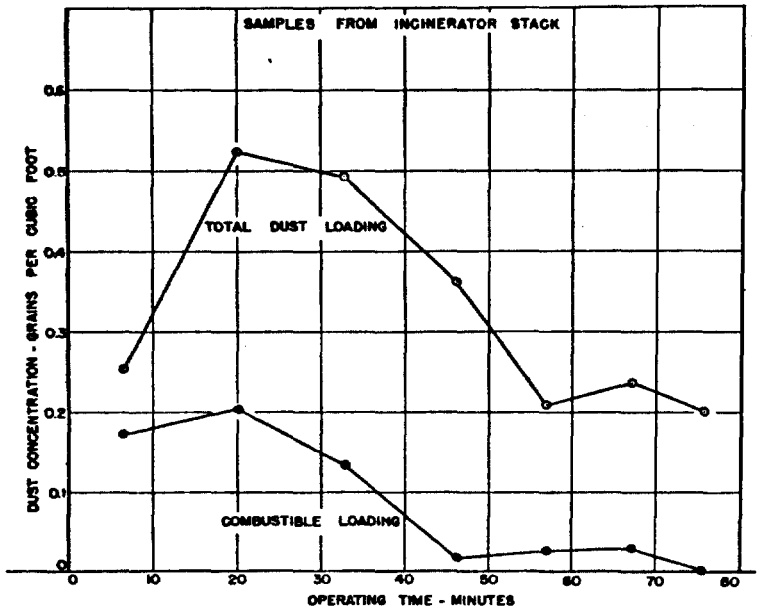

Fig. 8--Test Data, Test PH-18, 100 lbs. Sawdust in BOMAEC-100

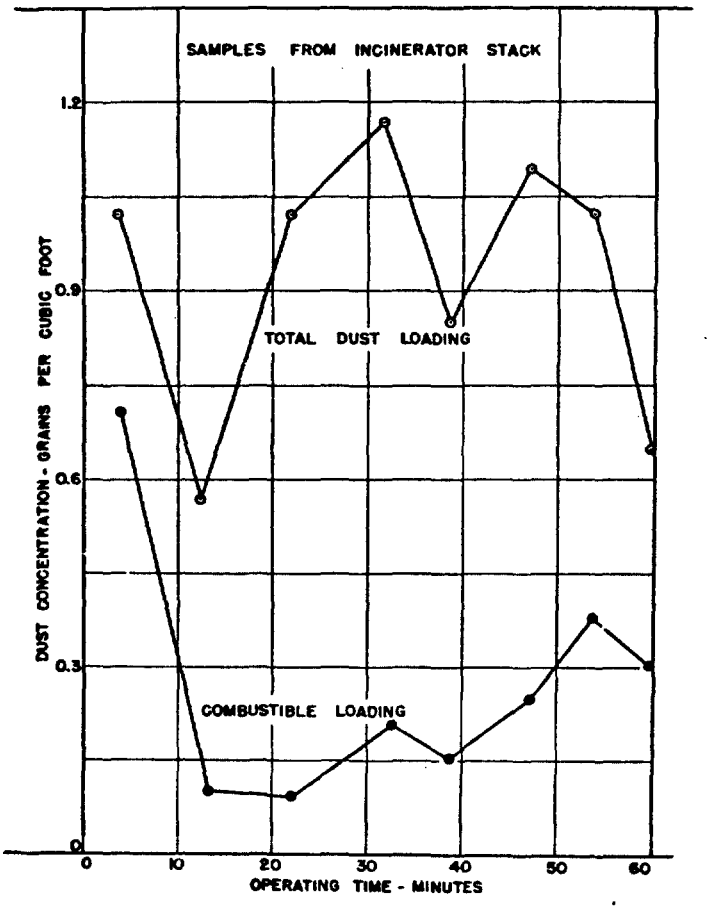

Fig. 9--Test PH-19, Office Waste, 15% Moisture, BOMAEC-100.

FURTHER STUDIES ON ELECTROSTATIC MECHANISMS OF AEROSOL FILTRATION

by

David M. Anderson and Leslie Silverman

Air Cleaning Laboratory
School of Public Health
Harvard University
Boston, Massachusetts

INTRODUCTION

At the Harvard School of Public Health, research on electrostatic mechanisms of aerosol separation has proceeded along three main lines. Packed fibrous beds have been studied to obtain the relation between aerosol and fiber charge, and the improvement in inherent filtration, i.e. the electrostatic efficiency. Fabric media have been studied to relate apparent surface charge on the fabric and collection improvement. Some preliminary studies of a more basic nature have been made to define coulombic, dielectrophoretic, image, and space charge forces operating between parallel plane and irregular surfaces.

The initial studies on the first two phases have been completed. Detailed descriptions of the study on fibrous beds are available in NYO reports (1,2,3,4) and in the open literature (5). Results of the investigations on fabric media have now been published (7,9) and will be expanded in an NYO report soon to be released (8). The third phase of study, basic forces, is being completed and will be described in a separate NYO report. It is the purpose of this paper to summarize very briefly the completed studies, to describe the current phase of research, and to indicate proposed future studies.

SUMMARY OF COMPLETED STUDIES

A. Fibrous Bed Studies

At the third Air Cleaning Conference the effects of aerosol charge on the efficiency of an uncharged fiber bed were reported (6). The apparatus (Figure 1) was described, which consisted of a spinning disc aerosol generator (used for generating methylene blue spheres, MMD = 2.0 μ, σ_g = 1.3), a wire-cylinder ionizer for aerosol charging, a test filter section which also served as the aerosol and fiber charge measuring device by using the Faraday ice-pail principle, sampling probes, and a blower. The same apparatus was used for determining the effects of fiber charge on an uncharged aerosol and the combined effects of both aerosol and fiber charge.

Using packed 50 μ glass fibers as the uncharged filter it was found that efficiency increased systematically with aerosol charge reaching a maximum at a value 2×10^{-5} statcoulombs/gm. (2000 e/part.). These results were independent of aerosol polarity. Tests using a negatively charged 70 μ saran fiber bed and an uncharged aerosol showed that filter efficiency increased smoothly with fiber charge to over twice the initial value at a fiber surface charge of 0.3 statcoulombs/cm.^{2}. With the aerosol and filter charged to opposite polarities, efficiency increased more rapidly. At comparatively high fiber surface charge (0.7 statcoulombs/cm.^{2}) however, aerosol charge became unimportant and filter charge determined the efficiency almost exclusively. In addition this study included preliminary investigations of the effects of fiber size, filtration velocity, and packing density on electrostatic efficiency and related tests on the effective life

of a charged fiber filter. The concept of "self-charging" filters was investigated and results using filtered air, room air, and a methylene blue aerosol at loadings of 1.0 mg./M^3, with velocities up to 360 fpm, showed no measurable electrification of 70 μ saran fibers.

B. Fabric Media Studies

In this phase of the over-all program a device was constructed in which a mechanically charged fabric surface was employed as the filtering medium for atmospheric dust. Figure 2 shows the final unit as it was developed into a two-stage cleaner. This unit consists of a lucite box, D, perforated on two sides and mounted vertically between two lucite rollers, E. The fabric to be tested was sewn in the form of an endless belt, F, and placed over the rollers thus enclosing the box. A small electric motor geared to the bottom roller caused the belt to travel around the box and also drove a counter rotating paddle, C, covered with a fabric which served to charge the belt by a contact-separation mechanism. This assembly was enclosed in a Masonite box, G, one face of which was cut in grid form and covered with a fabric, A, the same as that covering the paddle. This fabric surface was charged by the action of a windshield wiper blade, B, covered with the same fabric as the belt. Air flow was through the screen and then through the belt. The unit was tested by sampling at three points, upstream, interstage, and downstream. Efficiencies were computed using the stain density of the dust on Whatman No. 41 filter paper. Fabric surface charge was measured by a charge pick-up probe, developed by this laboratory. Aerosol charge was not controlled and ranged from an estimated average net charge of <1.0 to 45 electron units (positive) per particle (as measured in a Faraday cage system).

The fabrics tested in this unit included wool, resin-wool, saran, and orlon, in various combinations. The basic uncharged efficiency on atmospheric dust of the two-stage unit could be doubled by mechanically charging the fabrics by contact with other suitable fabric surfaces. It was shown that the electrostatic mechanism introduced by mechanical charging was not quite as beneficial as that produced by the action of a resinous additive. However, mechanical charging was accomplished at no change in resistance. Moreover, the magnitude of the improvement from mechanical charging was by no means maximized in these tests. In addition particle charging by the charged first stage was shown to occur and to aid collection when the second stage was uncharged but was found to be unimportant when the second stage was charged to a sufficient magnitude. (This is essentially the same conclusion reached in the independent packed fiber bed study just discussed.) Other tests showed that the efficiency due to electrostatic effects was inversely related to filtering velocity and directly proportional to the apparent surface charge generated on the fabrics. The magnitude of this charge was shown to be dependent on the fabric composition, type of charging action, and absolute humidity.

FUNDAMENTAL RESEARCH

Throughout the previous investigations there was a need for a more basic understanding of the fundamental mechanisms of electrostatic capture with regard to aerosols such as atmospheric dust possessing only natural charges due to their generation, and moving in the streamline flow range as occurs in the motion past fibers in both packed beds and fabrics. The literature on electrostatic separation is, unfortunately, sparse in these two areas, most of it concerning aerosols of high charge moving in turbulence. Retention time in an electrostatic field, field strength, field configuration, and position of the collection surface with respect to the aerosol, required further investigation. Therefore a study was initiated with atmospheric dust moving in streamline flow using a vertical parallel-plate type condenser unit, directly charged (Figure 3). This is the simplest orientation which may be handled theoretically. The unit consisted of a rectangular Masonite channel of variable width, 16" long, and 18" deep. The inner faces of the channel were removable. In the following tests polished aluminum sheets, and plates covered with a layer of "Metlon", an aluminum-polyethylene woven cloth, were used as the collecting faces in the channel, producing uniform and non-uniform fields respectively. These collecting faces were charged directly with a 20 kv power supply and the field strength measured by plate voltage and capacitance. In the case of the non-uniform fields, the "apparent" field strength was measured, which was accurate except at very short distances from the cloth surfaces. Atmospheric dust was used as the test aerosol and samples up- and downstream were again measured by stain density. A statistical method of

averaging results was developed since many factors influence any one stain measurement and since an important variable, aerosol charge, varied during the tests.

For charged particles moving between two flat charged plates two forces were considered operating, field forces and image forces. The field force is derived from the definition of an electric field and is characterized by

$$F_C = \mathcal{E} Q_p \qquad \text{Equation (1)}$$

The image force is due to the decreased energy in the weakened field surrounding the particle when it is near a conducting body, regardless of the potential of the conducting body. It can be thought of as a coulombic force of attraction due to a mirror image of the charge in the conducting body and in the case of an infinite plane is characterized by (10)

$$F_I = \frac{Q_p^2}{4y^2} \qquad \text{Equation (2)}$$

Because the aerosol tested was considered to consist of approximately equal numbers of particles of opposite sign, space charge effects were neglected. Calculations also showed that for the plate spacings used, diffusional forces are negligible. Because of the vertical orientation of the unit, gravity effects can also be neglected. The equation of motion between these plates for particles in the Stokes' Law range is therefore

$$m \frac{dV_y}{dt} + \frac{6\pi\mu r V_y}{1+A(L/r)} - \mathcal{E} Q_p - \frac{Q_p^2}{4}\left[\frac{1}{y^2} - \frac{1}{(Y-y)^2}\right] = 0 \qquad \text{Equation (3)}$$

The first term is the inertia force, the second is the particle drag, the third is the field force, and the fourth is the force due to images of the charged particle in both plates. The fourth term is actually only an approximation since the image charges themselves induce images in the opposite plate and these images

in turn produce further images in an infinite series. The image force as written contains only the first terms of these infinite series and is a good approximation since each succeeding term decreases by the square of a distance which itself becomes infinite.

By integrating the fluid velocity distribution for streamline motion between parallel plates, and combining the result with the solution of Equation 3 for field forces operating alone, an equation can be written for the stopping distance x_s traveled by a particle starting at $t = 0$; from the position $x = 0$, $y = y$ (any particle just entering the area between the plates) and arriving at the point $x = x_s$, $y = 0$ (being caught on the plate at distance x_s) (11):

$$x_s = \frac{6\pi\mu r V_{avg}(3Y_y^2 - 2y^3)}{Y^2 Q_p[1+A(L/r)]} \qquad \text{Equation (4)}$$

The precipitating efficiency of such a parallel plate device is the fractional air volume swept clean in the distance x_s. Since the aerosol is considered to consist of equal numbers of particles of both signs the total efficiency is the ratio of the air volume entering the unit out to point y to the total air volume. Integrating the velocity distribution again the efficiency is, for a variable distance y

$$\eta = \frac{3Y_y^2 - 2y^3}{Y^3} \qquad \text{Equation (5)}$$

Using equation 4 to determine the limiting distance y for $x_s = X$, i.e. the total plate length, and combining with equation 5, the over-all efficiency is expressed by

$$\eta = \frac{X}{Y V_{avg}} \left[\frac{\varepsilon Q_p (1 + A (L/r))}{6\pi\mu r}\right], \eta \leq 1.0 \qquad \text{Equation (6)}$$

The term in brackets is the so-called plate migration velocity. This equation agrees in form with those given elsewhere (15).

This equation is of limited application since it refers only to the field force operating between parallel charged plates oriented perpendicularly, with air flow in streamline motion and a homogeneous aerosol of uniform size and charge distributions. In the experimental tests field forces do not occur alone nor are the charge and size distributions of the aerosol uniform. It will serve for comparison purposes, however.

The equation of motion for particles moving due to image forces operating alone could not be solved by any of the classical methods of differential equations. The use of finite differences was attempted but the number of steps required became prohibitive. Its solution is now being attempted using an electronic analog computer.

In an irregular field, as produced by a charged rough surface, the field gradient $\partial \mathcal{E}/\partial_y$ is not constant as between parallel plates but is a function of the distance from the surface. In such a field a third force, dielectrophoresis, becomes operative, and is characterized by (12).

$$F_D = K \frac{(K_1 - K)}{(K_1 + 2K)} \quad \frac{(D_p{}^3)}{(8)} \mathcal{E} \frac{\partial \mathcal{E}}{\partial y} \qquad \text{Equation (7)}$$

This force is due to induction and attraction of electric displacement charges within the particle which tends to produce a dipole and occurs whether the particle is charged or not. The differential equation describing motion due to this force is complicated and can only be written for particular geometric shapes and orientations, and definitely not for the heterogeneous fields produced in these investigations. It will be noted, however, that the force is independent of particle charge and increases with particle size.

Figure 4 represents tests to determine the effect upon efficiency of field strength at constant velocity and plate spacing. Curve 1 shows the effect of a uniform field. The relation is nearly linear up to a limiting field strength of approximately 13 dynes/statcoulomb after which a maximum efficiency, 80%, is reached. The heterogeneous field, Curve 2, shows a larger effect at the same apparent field strength due to the added dielectrophoretic force described in Equation 7 but also reaches a maximum at the same efficiency. This added efficiency is at no extra expenditure of power and shows the value of even a slightly heterogeneous field (See White (13), p. 936).

It will be noted that both curves shown an intercept at zero field strength. This is attributed to image forces which are now being investigated separately. Curve 3 is a plot of equation 6 starting at the intercept and using the previously measured average net Q_p of 25 electron charges. Since efficiency was measured with a stain technique rather than a count method, and since aerosol size and charge characteristics were variable, exact analytical comparisons of the data and the theory are not warranted. However, in spite of these limitations, it is obvious that an average Q_p of 25 e is notrealistic. Curve 4 is the theoretical count efficiency which most closely fits the experimental data and is for a uniform aerosol with an average Q_p of 0.4 e. The high measured charge is probably due to relatively few particles of high Q_p. The actual aerosol probably possesses a mean Q_p much nearer 0.4 e. The assymptotic efficiency of 80% is attributed to the removal of all charged particles which can significantly influence a stain density measurement.

Figure 4 reveals that at a low velocity a condenser-type apparatus will give high stain efficiencies on a naturally-charged aerosol

such as atmospheric dust without aerosol charging by ionization as in two-stage electrostatic precipitators. The field strength necessary for these high efficiencies (10 statvolts/cm.) is about 40% of that used in the second stage of the conventional two-stage precipitator (Westinghouse Precipitron). With a heterogeneous field the high efficiency (80%) is possible at even lower field strengths. For removal of uncharged particles (20% by stain for atmospheric dust) the heterogeneity must be more intense than that produced by an irregular semi-plane surface i.e. the field gradient $\partial E/\partial y$ must be greater for dielectrophoresis to become significant.

Figure 5 presents the results of tests to determine the effect of velocity and plate spacing on collection. Curve 1 is the experimentally determined relationship at E= 11.7 dynes/statcoulomb, Y = 4.44 cms.

Curve 3 shows the experimental values at the same field strength, 11.7 dynes/statcoulomb, but at a closer place spacing 1.91 cms. Both curves indicate that stain efficiency falls off rapidly with increasing velocity. For decreasing plate spacing this rate of fall-off becomes less rapid. At the same time image forces increase at a rate proportional to the square of the spacing (see equation 2). Therefore it appears that if plate spacing is further decreased high stain efficiencies will be obtained at velocities which will be more in line with practical values. The spacing must, of course, not approach values which will make pressure loss prohibitive.

Figure 6 presents the experimental results for the conditions of increased field strength, E = 17.9 dynes/statcoulomb, and Y = 1.91 cm. Superimposing Curve 1 of this figure on Curve 2 of Figure 5 it is found that the effect of increasing field strength is

significant above 150 fpm but below this velocity (and at this spacing) this 50% increase in field strength seems to affect the efficiency very little. This is to be expected since the difficult-to-assess areas are in the steep portions of these curves where efficiency is affected by velocity to the greatest extent. At low velocities the effect of field strength is actually considerable as was shown in Figure 4.

Curve 3 shows the effect of introducing a slight heterogeneity to the field form in the manner described previously. The results so closely parallel the uniform field that the two curves could actually be drawn as one. At low velocities, nevertheless, the effect of a slight heterogeneity is apparent as was shown in Figure 4. Curve 4 is a plot of results of tests where the field strength was zero, the "base-efficiency" of the unit. The points represent two plate spacings, 1.91 and 4.44 cms., between which no significant difference in results were noted. There is a wide spread in the data, and, in fact, above 50 fpm the curve could probably have been plotted at zero efficiency rather than at 5.0%. Below 50 fpm, however, there is a definite increase to a significant efficiency as velocity is decreased. This efficiency is attributed to image forces.

Curve 2 represents the theoretical curve of best fit using equation 6 and the image force efficiency from curve 4, i.e. $\eta_T = \eta_I + \eta_F$ where η_T is the total efficiency, η_I is the image force efficiency from the experimental curve 4, and η_F is the field force efficiency determined from equation 6. It is plotted only up to 200 fpm where flow becomes turbulent (based on a Reynolds number criterion of 2000) and where equation 6, therefore, ceases to apply. The shape of this curve is a slightly modified equilateral hyperbola. It is plotted for an average Q_p of 0.9 e

which is in the same order of magnitude as the Q_p determined from Figure 4. The limitations in the stain efficiency technique and the variability of aerosol properties prevent an analytical comparison of the curves, as mentioned above. Nevertheless curves 1 and 2 do possess some degree of similarity in shape.

Over-all conclusions from this study indicate: 1) high stain efficiencies on a naturally-charged aerosol are possible by using a condenser type apparatus at field strengths materially smaller than those normally used in the collecting stage of electrostatic precipitators; 2) low velocities and small plate spacings are necessary for optimum performance; 3) at low velocities a slight heterogeneity of the field form increases efficiency significantly at no increase in energy but a more intense field gradient than that produced by a rough plane surface is necessary to capture uncharged particles by dielectrophoresis; 4) also at low velocities image forces become important as a precipitating mechanism; 5) the average net Q_p of atmospheric dust appears to be in the order of one electron charge per particle (positive) but not all particles which influence a stain density measurement are charged, i.e. roughly 20% are uncharged.

CURRENT RESEARCH

The next line of study undertaken has been a more detailed investigation of image forces. This phase is currently in progress. The over-all purpose of the electrostatic studies at Harvard has been the optimum utilization of naturally occurring or mechanically produced electrostatic charges for air cleaning, thus doing away with power supplies and expensive auxiliary electrical equipment. As was shown above, significant image force effects are possible with naturally charged aerosols. Consequently a study has been initiated to investigate this mechanism in a fundamental manner. Determining the value of this separating force resolves essentially to the solution of the following differential equation written for the image force operating alone in a grounded parallel conducting plate channel at distances of less than Y/4, where Y is the plate spacing:

$$m \frac{dV_y}{dt} + \frac{6\pi\mu r V_y}{1+A(L/r)} - \frac{Q_p^2}{4y^2} = 0 \qquad \text{Equation (8)}$$

This is Equation 3 rewritten for the image force due to one plate alone for the condition where this force becomes controlling, i.e. where the force due to the other plate becomes negligible. In cases of collection by convex shaped targets such as fibers or spheres the image force will be less than that given by the third term of this equation (10). Concave shaped targets such as the inside wall of a hollow cylinder will produce an image force greater than the third term of this equation (14) but the representation of this force becomes more complicated. Therefore a parallel plate system was chosen as the case to be studied since the image force is of intermediate magnitude and can be represented in the simplest manner mathematically.

Equation 8 appears to be simple in form but unfortunately cannot be solved by classical mathematics. All obvious substitutions of variable reduce the equation to non-separable, first order, second degree, or non-separable, second order, third degree forms which cannot be solved. The use of operational calculus and the Picard method of general solutions to differential equations are also of no avail. A finite difference solution is possible but at distances of $y > 10^{-4}$ cm. the number of steps becomes prohibitive, e.g. for $y = 10^{-3}$ cm., the number of steps required is 10^{15}. A graphical method has been developed which may lead to a solution.

The validity of any deduced mathematical solution must necessarily be checked by experiment. Figure 7 is a schematic representation of the unit now being tested to determine the value of the image force experimentally. The aerosol generator, A, consists of a $3\frac{1}{2}$" diameter brass disc driven by a variable speed motor with a maximum speed of 3800 rpm. A 0.1% methylene blue in alcohol solution is fed from a constant head tank through a hypodermic needle onto the center of the disc and the aerosol is produced as droplets are centrifuged off the disc and the alcohol evaporates. The aerosol resulting consists of uniform solid spheres of 2.4 μ mass median diameter and a $\sigma_g = 1.3$. The aerosol is charged by an ion current produced in the wire and cylinder ionizing section, B. Ion currents are measured by a microammeter and voltages by a kilovoltmeter in parallel with the power supply. The upstream sample is drawn through a millipore filter E, mounted in a Faraday cage, D. Volume rates of flow are from 1 - 30 lpm. As the charged aerosol is caught by the millipore the net charge is measured by the induced voltage on an electrostatic voltmeter, the entire system capacitance being known. The concentration of

aerosol is measured colorimetrically by dissolving the sample and millipore in acetone. This upstream sample then gives the weight concentration and net charge of the aerosol which enters the test section, F. This section is constructed of two pieces of 18 gauge stainless steel which form a rectangular channel 36" long and 12" wide and of variable thickness. This conducting channel is grounded. On the center of one face of this channel 1" steel circles, G, have been punched out every 6 inches such that the smooth discs may be removed. As the aerosol traverses the test section it is hoped that sufficient aerosol will be deposited on the walls by the image force to give the gradient of concentration with length of path, by analyzing for the aerosol deposited on these sampling discs. The aerosol then passes to the downstream sampler, H, and is analyzed for weight concentration colorimetrically in the same way as the upstream sample, thus giving the over-all test section efficiency. Flow rates through H vary from 1 - 30 lpm thus varying the velocity in the test section. The entire flow through the unit passes through the sampling filters and therefore no external air mover is necessary. The dimensions of the test section have been so chosen to allow enough test aerosol for weight and charge analyses to move at the low velocities ($<$10 fpm) required to determine the effect of the image force.

At this point it should be noted that with a unipolar aerosol such as is produced by this test setup an additional space charge effect will occur simultaneously with the image force. Therefore, appropriate corrections will be made in the experimental results. No tests have yet been made with this unit.

PROPOSED RESEARCH

Several lines of study have been proposed for future work. The most promising appears to be the evaluation of the electrostatic properties of fluidized beds as they effect aerosol filtration. In particular the use of granular solids capable of triboelectrification appears reasonable., These particles would become charged by the natural collisions occurring as they become fluidized and would present naturally charged targets for aerosol capture by coulombic and dielectrophoretic forces in addition to the image forces due to the aerosol itself. This will be the next main line of study on electrostatic mechanisms at Harvard.

LEGEND

1. AEROSOL GENERATOR
2. STAIRMAND DISC
3. DIFFUSER SCREEN
4. IONIZER SECTION
5. SAMPLING SYSTEM
6. FILTER HOLDER - FARADAY CAGE
7. HI-VOL BLOWER
8. POWERSTAT UNIT
9. D.C. POWER SUPPLY
10. SHALLCROSS D.C. KILOVOLTMETER
11. MICROAMMETER
12. ELECTROSTATIC SHIELD
13. PSYCHROMETER

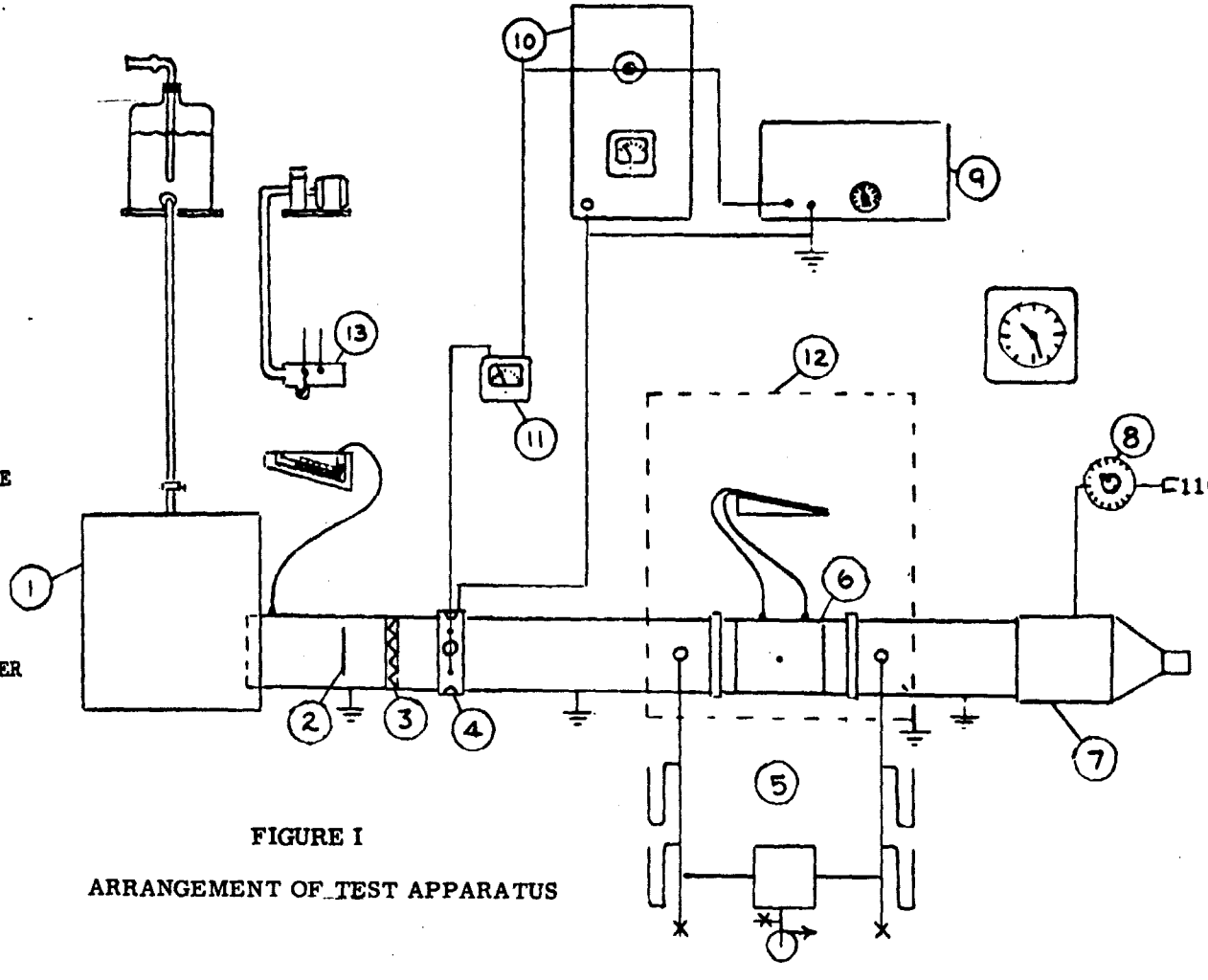

FIGURE I

ARRANGEMENT OF TEST APPARATUS

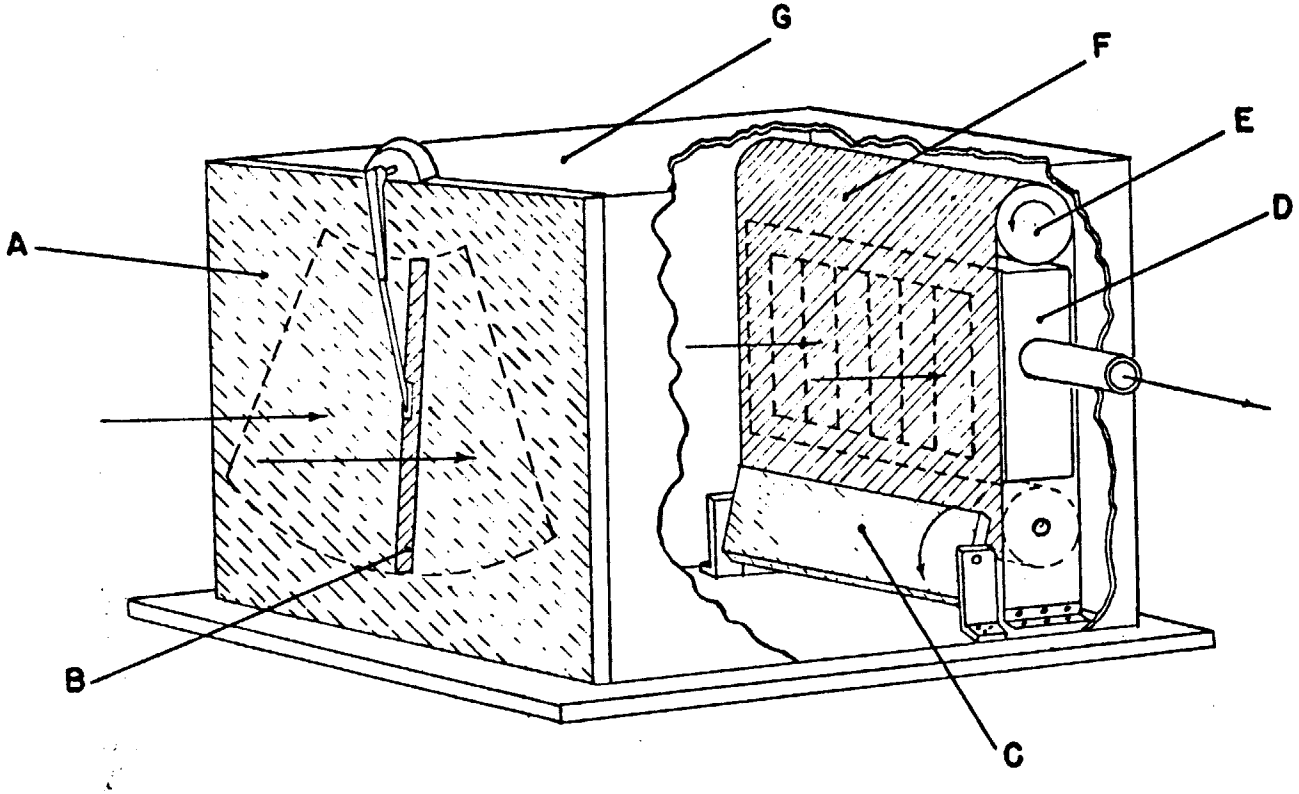

A – FABRIC A SCREEN
B – FABRIC B COVERED WINDSHIELD WIPER BLADE
C – FABRIC A COVERED PADDLE
D – LUCITE BOX
E – LUCITE ROLLER
F – FABRIC B BELT
G – MASONITE BOX

FIGURE II

MECHANICALLY CHARGED FABRIC FILTER – TWO STAGE

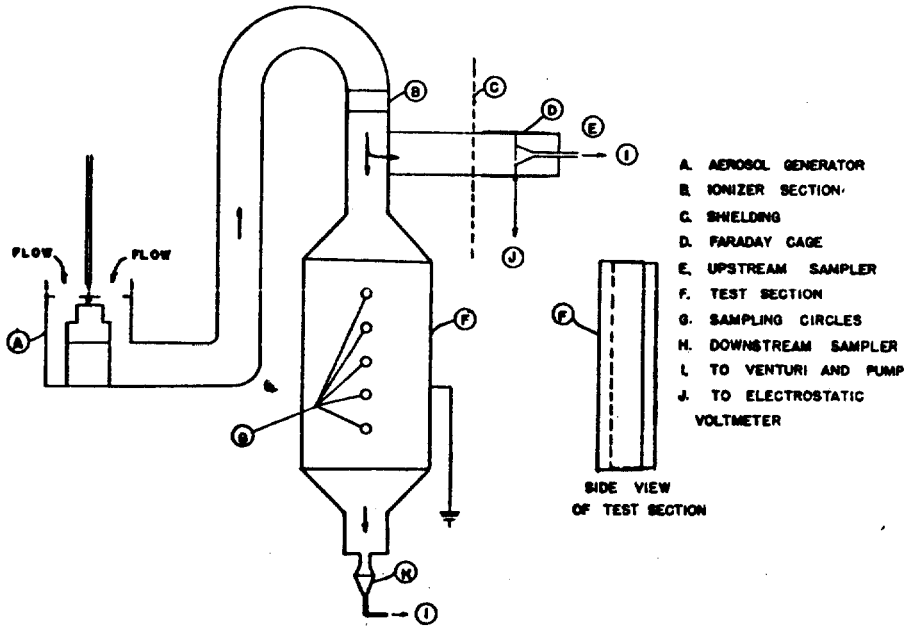

SCHEMATIC ARRANGEMENT OF APPARATUS FOR IMAGE FORCE STUDY

FIGURE III

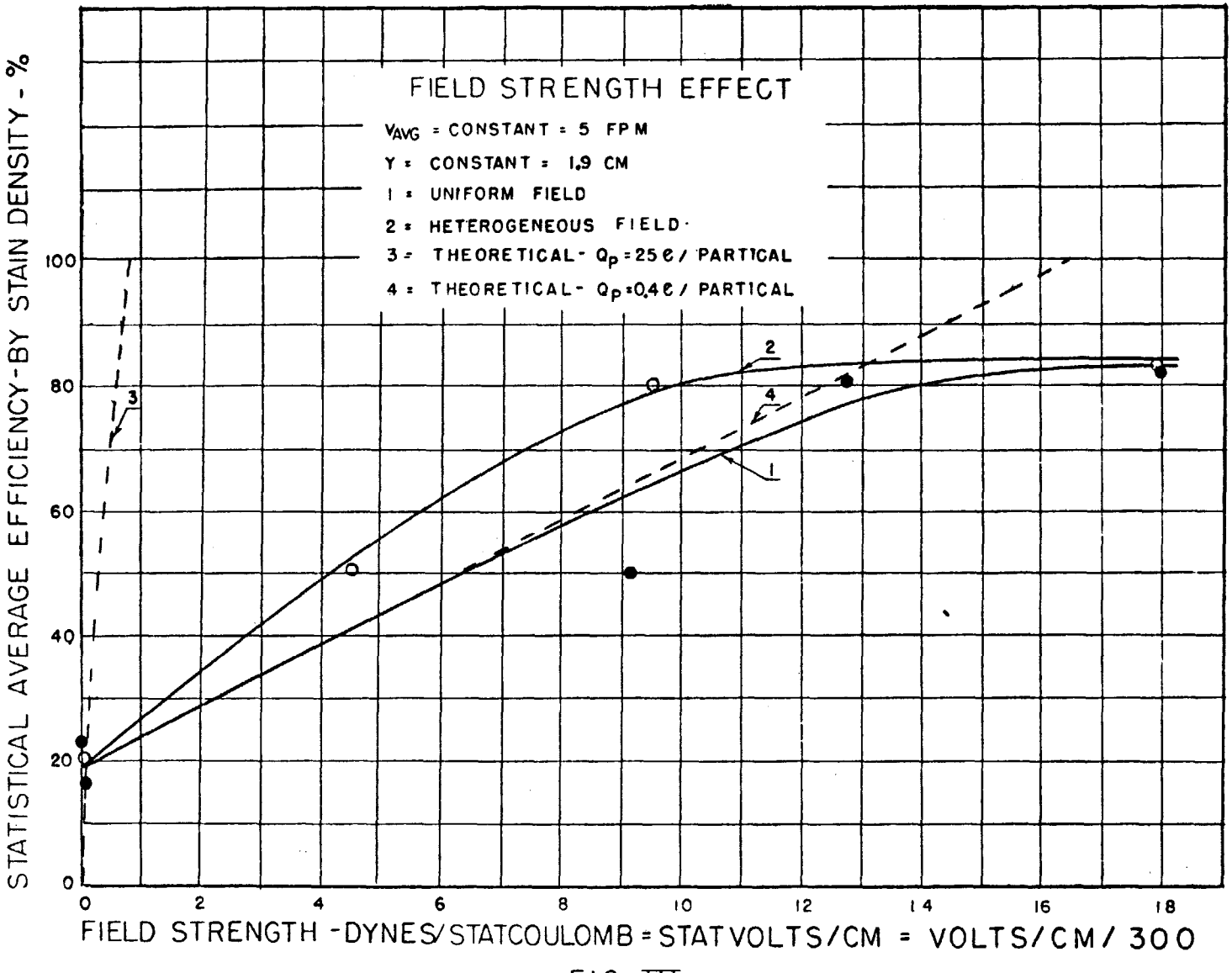
FIELD STRENGTH EFFECT
VAVG = CONSTANT = 5 FPM
Y = CONSTANT = 1.9 CM
1 = UNIFORM FIELD
2 = HETEROGENEOUS FIELD
3 = THEORETICAL - Qp = 25 e / PARTICAL
4 = THEORETICAL - Qp = 0.4 e / PARTICAL
STATISTICAL AVERAGE EFFICIENCY-BY STAIN DENSITY - %
0
20
40
60
80
100
0
2
4
6
8
10
12
14
16
18
FIELD STRENGTH - DYNES/STATCOULOMB = STATVOLTS/CM = VOLTS/CM / 300

FIG. IV

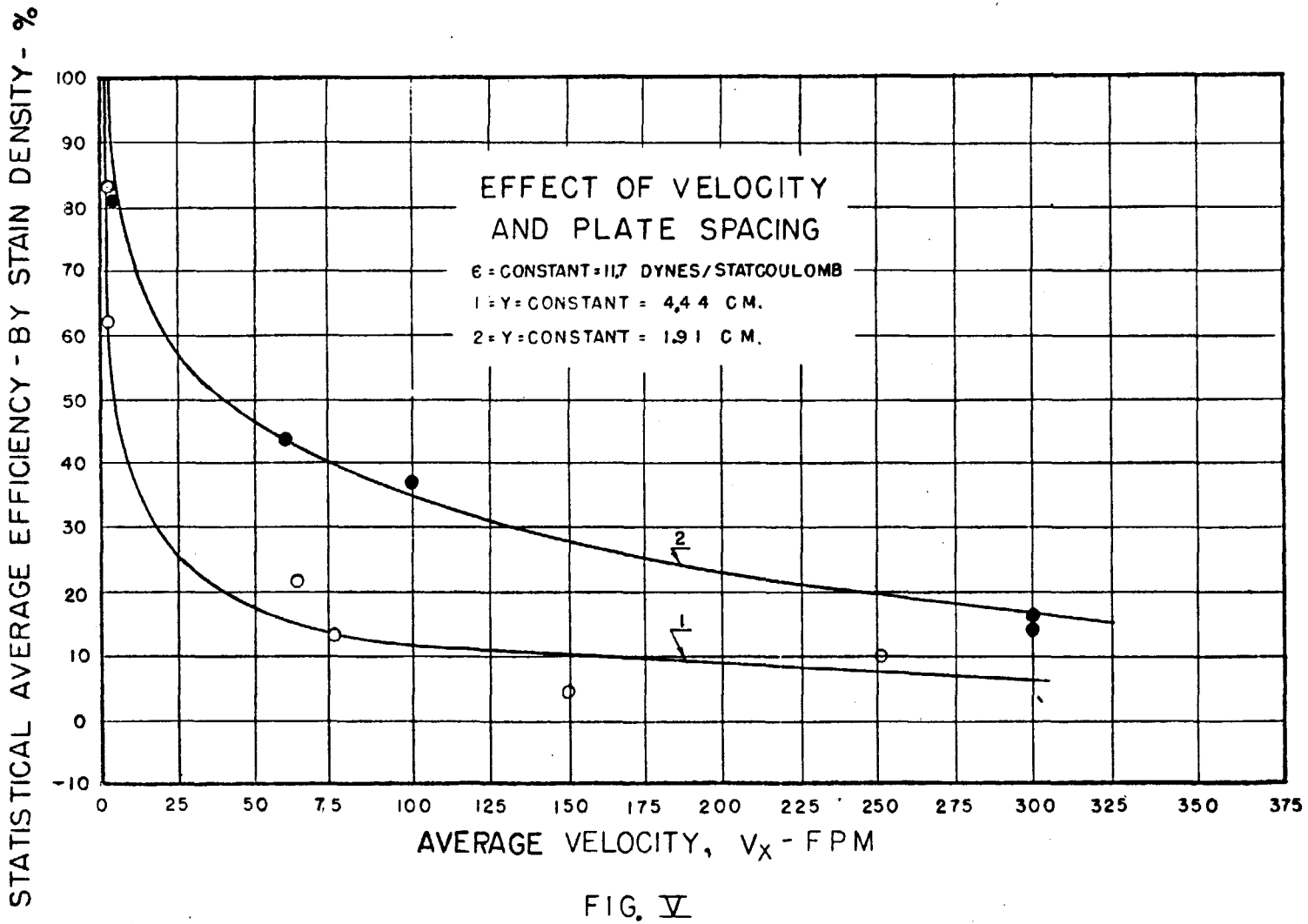
EFFECT OF VELOCITY
AND PLATE SPACING
ε = CONSTANT = 11.7 DYNES/STATCOULOMB
1 = Y = CONSTANT = 4.44 CM.
2 = Y = CONSTANT = 1.91 CM.
STATISTICAL AVERAGE EFFICIENCY - BY STAIN DENSITY - %
AVERAGE VELOCITY, V_X - FPM
100
90
80
70
60
50
40
30
20
10
0
-10
0
25
50
75
100
125
150
175
200
225
250
275
300
325
350
375
1
2

FIG. V

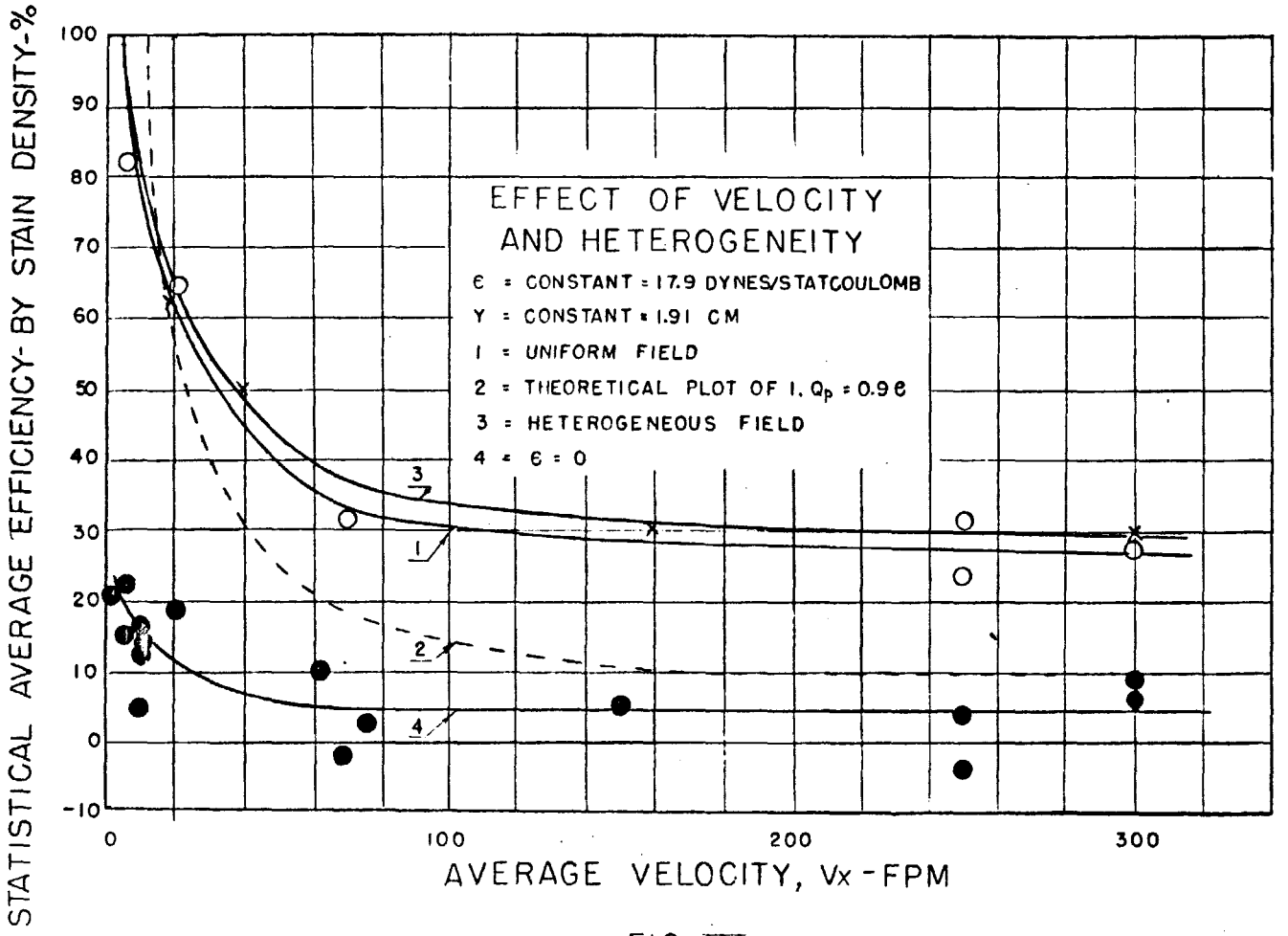
EFFECT OF VELOCITY
AND HETEROGENEITY
ε = CONSTANT = 17.9 DYNES/STATCOULOMB
Y = CONSTANT = 1.91 CM
1 = UNIFORM FIELD
2 = THEORETICAL PLOT OF 1. Q_p = 0.9 ε
3 = HETEROGENEOUS FIELD
4 = ε = 0
STATISTICAL AVERAGE EFFICIENCY- BY STAIN DENSITY-%
AVERAGE VELOCITY, Vx - FPM
100
90
80
70
60
50
40
30
20
10
0
-10
0
100
200
300

FIG. VI

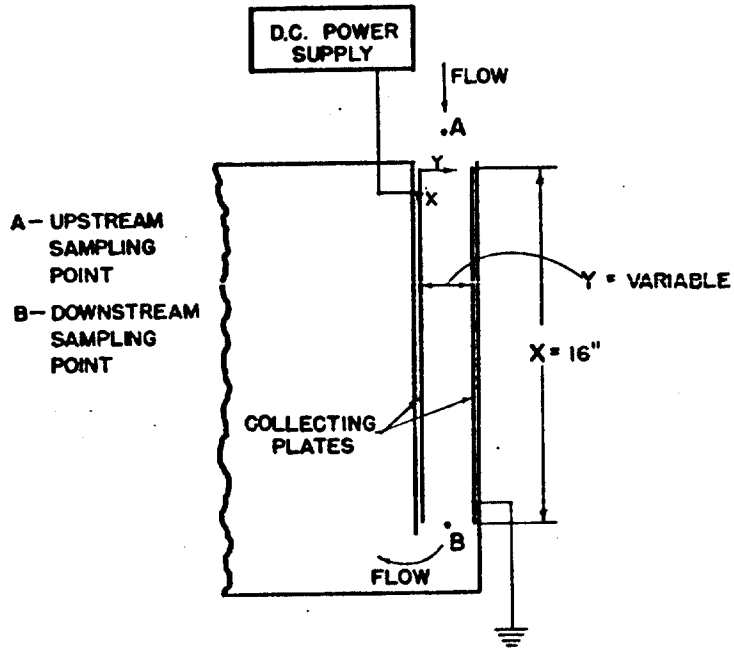

SECTIONAL SCHEMATIC OF PARALLEL PLATE DEVICE FOR ATMOSPHERIC DUST

FIGURE VII

NOMENCLATURE*

A = Cunningham correction factor, dimensionless

F_C = coulombic force in an electrostatic field, dynes

F_D = dielectrophoretic force in a divergent electrostatic field, dynes

F_I = force due to an electric image, dynes

K = dielectric constant of fluid, dimensionless

K_1 = dielectric constant of particle, dimensionless

L = mean free path of air molecules, cm.

MMD = mass median diameter, microns

Q_p = particle charge, statcoulombs

V_{avg} = average fluid velocity parallel to plates, cm./sec.

V_y = velocity perpendicular to plates at point y, cm./sec.

X = length of plates in direction of flow, cm.

Y = plate spacing, cm.

m = mass of aerosol particle, gm.

r = radius of aerosol particle, cm.

x = distance along plates in direction of flow, cm.

x_s = stopping distance of particle starting at $x = 0$ and $y = y$ to point $x = x_s$, $y = 0$.

y = perpendicular distance from either plate, cm.

$\mathcal{E}$ = electrostatic field strength, dynes/statcoulomb

η = fractional portion of aerosol collected, dimensionless

σ_g = geometric standard deviation, dimensionless

μ = fluid viscosity, poises

* Unrationalized cgs system of units used

LITERATURE CITED

A. On Fibrous Beds

1. First, M. W., Silverman, L., et al., "Air Cleaning Studies - Progress Report, Feb. 1951 - June 1952", U. S. Atomic Energy Commission, NYO-1586, Harvard University, Dec. 16, 1952, pp. 91-105.

2. First, M. W., Silverman, L., et al., "Air Cleaning Studies - Progress Report, July 1952 - June 1953", U. S. Atomic Energy Commission, NYO-1591, Harvard University, Aug. 5, 1954, pp. 16-26.

3. Dennis, R., Silverman, L., et al., "Air Cleaning Studies - Progress Report, July 1953 - June 1954", U. S. Atomic Energy Commission, NYO-4608, Harvard University, Jan. 15, 1956.

4. Rossano, Jr., A. T. and Silverman, L., "Electrostatic Mechanisms in Fiber Filtration of Aerosols," U. S. Atomic Energy Commission, NYO-1594, Harvard University, May 11, 1955.

5. Rossano, Jr., A. T. and Silverman, L., Heating and Ventilating, 51, 102-8 (May 1954).

6. "Third Atomic Energy Commission Air Cleaning Conference", U. S. Atomic Energy Commission, WASH-170, Division of Engineering, Washington, D.C. Nov. 1954. (Not for public distribution)

B. On Fabric Media

7. Silverman, L., Conners, Jr., E. W., and Anderson, D. M., Ind. Eng. Chem., 47, 952 (1955).

8. Silverman, L., Anderson, D. M., and Conners, Jr., E. W., "Mechanical Electrostatic Charging of Fabrics for Air Filters and Related Fundamental Studies", U. S. Atomic Energy Commission, NYO-4609, Harvard University. (To be released)

9. "Second Air Cleaning Seminar", U. S. Atomic Energy Commission WASH-149, Ames Laboratory, Ames, Iowa, March 1954. (Not for public distribution)

C. On Fundamental Mechanisms - Specific

10. Gilbert, N. E., "Electricity and Magnetism", revised ed., MacMillan Co., New York, 1941.

11. Daniel, J. H. and Brackett, F. S., J. Appl. Phys., 22, 542 (1951).

12. Pohl, H. A., J. Appl. Phys., 22, 869-71 (1951).

13. White, H. J., Ind. Eng. Chem., 47, 932 (1955).

14. Peck, E. R., "Electricity and Magnetism," McGraw-Hill Book Co., N.Y., 1953.

15. Perry, J. H., Ed., "Chemical Engineers' Handbook," p. 1040, 3rd ed., McGraw-Hill Book Co., N.Y., 1950.

HIGH TEMPERATURE FILTRATION STUDIES WITH MINERAL WOOL

by
Leslie Silverman, W. David Small and Charles E. Billings
Harvard School of Public Health
Department of Industrial Hygiene
55 Shattuck Street
Boston 15, Massachusetts

The research discussed below has been sponsored since 1953 by the American Iron and Steel Institute through its Subcommittee on Air Pollution Abatement. Although this study is primarily concerned with a solution to air pollution problems created in the open hearth steel making process, the results obtained may be successfully applied to problems in the AEC; particularly the cleaning of high temperature gases evolved from reactors and from incineration of radioactive waste materials. The degree of cleaning of open hearth gases is obviously not as severe as required by the AEC in most instances but the development of a low cost device could have application for some AEC problems. In many instances a roughing filter of the type to be discussed might be advantageously used when followed by a higher efficiency filter.

Particulate loadings are much higher in exhaust gases from the open hearth furnace than would ordinarily be expected from most AEC activities, ranging from less than 0.1 to greater than 2.0 grains per cubic foot (STP). The aerosol is composed of fine particles of iron oxide ($<0.1\ \mu$), created by the molten steel bath, contained in a high temperature gas stream (500 to 1500°F). The general aspects of steel process needs in gas cleaning indicate a cleaner which will prevent the obscuring of visibility and is low in both capital and operating costs. To date the only acceptable method for open hearth furnace fume removal has been electrostatic precipitation. Because of their cost, precipitators have only been applied where public relations demand the expenditure. About three tons of iron

oxide may be recovered from a typical 250 ton furnace (per heat) during the production of 750 to 900 tons of steel per 24 hour day. Recovery value is negligible but a nuisance problem is created since the fume is of such a fine size that it has high light obscuring properties. Some of it may subsequently agglomerate and produce some settled dust in the nearby neighborhood. The problem, then, consists of removing economically large quantities of fine particles from high gas volumes at high temperature.

The study has been divided into two phases. First, a study of agglomeration has been undertaken since freshly formed metallic fumes in high concentration can be shown to flocculate and aggregate rapidly. Knowing this fact it was conjectured that perhaps the particle size could be increased to a point where simpler collection methods might be applicable.

The second phase of the program is to develop a cleaner simple in principle, design and operation, capable of withstanding high temperatures continuously. Because it is low in cost and has proven successful on a laboratory basis for gas mask filters, we studied mineral or slag wool as a fibrous medium. This material is a by-product of the steel mill blast furnace, and is readily obtained in bulk since it is widely used for insulating purposes. It is produced by blowing or spinning molten slag (or rock) with steam or air into refractory fibers with a mean size of approximately 4 microns costing approximately $0.01 per pound.

Studies by the Chemical Warfare Service and others in World War II showed that special finer fibers could be made but these would be higher in cost.

The apparatus shown in Figure 1 was used to study filtration characteristics of layers of various thicknesses and densities of

commercial slag wool fibers formed into 6 inch diameter filter pads. An iron oxide fume was generated by burning iron powder in an air-oxygen-acetylene flame, or by feeding iron carbonyl vapor into the flame. An electron photomicrograph of fume particles is shown in Figure 2. Although these are from an actual open hearth furnace, the fume from burning iron carbonyl was found to be comparable in size. Resistance characteristics of the filters were determined as shown in Figure 3. It was found that the optimum thickness and density for a desired resistance of 2 inches of water is approximately 1 inch and 5 pounds per cubic foot, respectively. Figure 3 indicates that the resistance varies linearly with velocity and also increases with higher temperature due to the gas viscosity increase. The velocities to be used in slag wool filtration for steel industry gas cleaning purposes are far greater than those used in AEC applications except for precleaning. In order to minimize the size of equipment due to space limitations a filtration velocity of at least 100 feet per minute is necessary. A typical 250 ton open hearth furnace produces 25,000 cfm (STP) of gas which is increased to greater than 50,000 cfm at the temperatures existing in the open hearth (>500°F).

It was found from these and other laboratory studies that slag wool filters will collect from 80 to 95 per cent of the fine iron oxide fume, at temperatures of 500 to 1000°F, and at filtering velocities of 100 to 200 feet per minute.

Investigations of the effects of time and dust loading on the resistance of the filter have been made with the laboratory fume and also with actual furnace fumes in the field. These have indicated that the slag wool filter (of 1 inch thickness and 5 pounds per cubic foot packing density) will recover about 2.5 per cent of its initial weight per 1 inch rise in resistance. To keep the filter resistance

within reasonable power limits it should not exceed 4 inches of water. Its initial value is between 1 and 2 inches. For an allowable resistance rise of 2 inches of water, the filter will then collect 5 pounds of fume per 100 pounds of fiber. Higher recovery percentages were obtained in the field indicating that coarser material was present. This appreciably raised the weight of the collected fume per 100 pounds of fiber.

It was apparent that it would be uneconomical to use slag wool as a filter for one pass use. Studies were made with regard to washing and reclaiming the fiber. The method selected for washing also was ideal for re-establishing the filter. Laboratory studies (later confirmed in the field) have indicated that by washing and reusing the wool, approximately 8 to 10 re-uses could be made before the fiber was no longer satisfactory. This increases utilization to about 50 pounds of fume per 100 pounds of fiber. In practice it is best to add 10 per cent new fiber in each wash cycle. This replaces the fiber reduced to brokem fragments by the recycling. The iron oxide fume, slag wool shot and broken fibers were easily removed in the washing, the rejected material settling to the bottom of a decantation tank.

Figure 4 shows the basic principle of the continuous slag wool filter developed at Harvard. The fibrous material forms a continuous filter pad which is passed through the furnace gases and removes the fume. The collected fume and slag wool are discharged into a wash tank where it is prepared for re-use. A pilot unit has been developed based on this design with a capacity of approximately 500 cubic feet of gas per minute. During the past winter, the method has been successfully tested on a typical open hearth furnace at a steel mill. Another filter is being constructed incorporating design changes suggested by the initial pilot unit.

The possibility of causing the fine iron oxide particles to

agglomerate to a larger size is being investigated. A longer path is provided by passing the gas through a rotating screw flight. Additional turbulent and thermal forces can be controlled by counter-rotating the screw and cooling the walls and shaft. With diffusion this should enhance the coagulation to a certain extent. The screw can also be provided with hoppers to take advantage of whatever inertial collection occurs. Present studies are concerned with developing air flow equations to predict the pressure loss characteristics of screws under various cooling and rotational conditions. Background efficiency data have also been obtained on iron oxide fume. Methods for measuring aerosol agglomeration are currently being investigated.

It is expected that a combination of the agglomeration and filtration techniques indicated above will lead to a compact gas cleaning unit to effectively remove 90 to 95 per cent of fine metal oxide fumes at low cost.

Additional information on this project has been published at greater length and is available upon request.

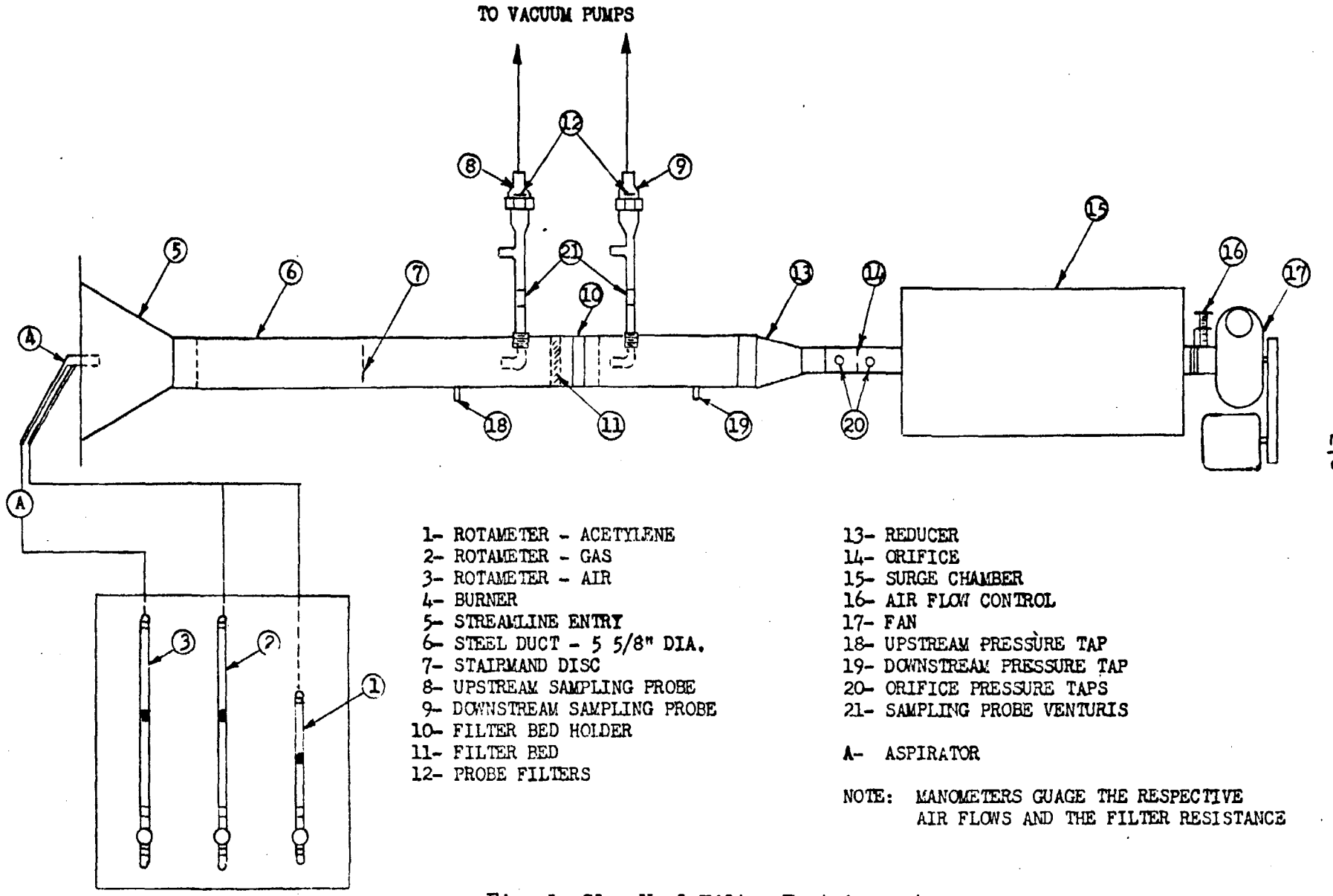

1- ROTAMETER - ACETYLENE
2- ROTAMETER - GAS
3- ROTAMETER - AIR
4- BURNER
5- STREAMLINE ENTRY
6- STEEL DUCT - 5 5/8" DIA.
7- STAIRMAND DISC
8- UPSTREAM SAMPLING PROBE
9- DOWNSTREAM SAMPLING PROBE
10- FILTER BED HOLDER
11- FILTER BED
12- PROBE FILTERS
13- REDUCER
14- ORIFICE
15- SURGE CHAMBER
16- AIR FLOW CONTROL
17- FAN
18- UPSTREAM PRESSURE TAP
19- DOWNSTREAM PRESSURE TAP
20- ORIFICE PRESSURE TAPS
21- SAMPLING PROBE VENTURIS

A- ASPIRATOR

NOTE: MANOMETERS GUAGE THE RESPECTIVE AIR FLOWS AND THE FILTER RESISTANCE

Fig. 1--Slag Wool Filter Test Apparatus.

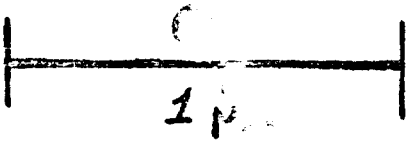

Fig. 2--Electron Photomicrograph of Hot Metal Open Hearth Furnace Fume, Taken before Waste Heat Boiler (X50,000).

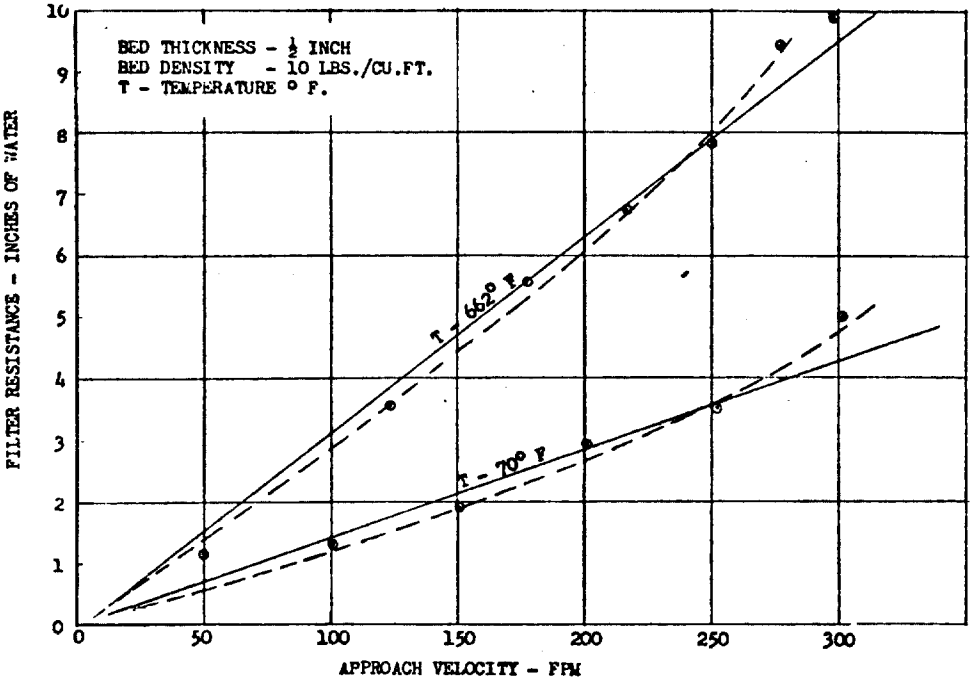

Fig. 3--Effect of Temperature on Filter Resistance.

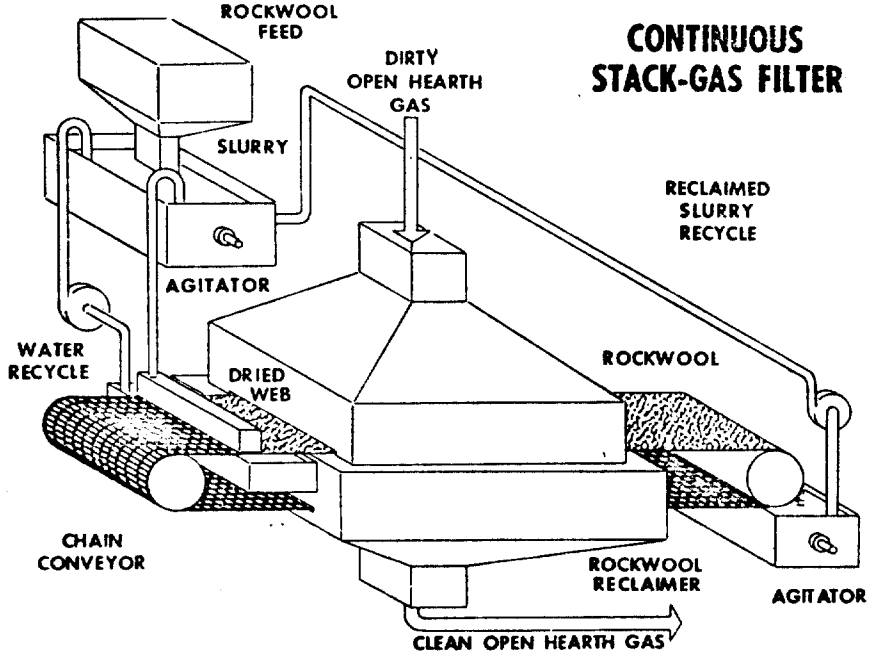

Fig. 4--Schematic Drawing of Continuous Slag Wool Stack Gas Filter Unit Showing Principle of Method.